

1
2
3
4
5
6
7
8
9
10
11
12
13
14
15
16

This manuscript is a non-peer review preprint that has been submitted to *Frontiers in Climate* on 27th November 2023. Subsequent versions of the manuscript might have different content.

17 **A Review of Measurement for Quantification of Carbon Dioxide** 18 **Removal by Enhanced Weathering in Soil**

19

20 **Matthew O. Clarkson¹, Christina S. Larkin¹, Philipp Swoboda¹, Tom Reershemius², T. Jesper**
21 **Suhrhoff^{2,3}, Cara N. Maesano⁴, James S. Campbell⁵**

22 ¹InPlanet GmbH, Heinrich-Geißler-Straße 20, 80939 München

23 ²Department of Earth and Planetary Sciences, Yale University, New Haven, CT, United States
24 of America

25 ³Yale Center for Natural Carbon Capture, Yale University, New Haven, CT, United States of
26 America

27 ⁴RMI, 22830 Two Rivers Road, Basalt, CO 81621, USA

28 ⁵Research Center for Carbon Solutions, Heriot-Watt University, Edinburgh, EH14 4AS, UK

29

30 *** Correspondence:**

31 Corresponding Author

32 matthew.clarkson@inplanet.earth

33 **Keywords: enhanced silicate weathering, negative emissions technologies, climate**
34 **change mitigation, carbon mineralization, MRV**

35 **Abstract**

36 All pathways which limit global temperature rise to $<2^{\circ}\text{C}$ above pre-industrial temperatures now
37 require carbon dioxide removal (CDR) in addition to rapid greenhouse gas emissions reductions.
38 Novel and durable CDR strategies need to rapidly scale over the next few decades in order to reach
39 Paris Agreement Targets. Terrestrial enhanced weathering (EW) involves the acceleration of natural
40 weathering processes via the deployment of crushed rock feedstocks, typically Ca- and Mg-rich
41 silicates, in soils. While models predict this has the potential to remove multiple gigatonnes of CO_2
42 annually, as an open-system pathway, the measurement (monitoring), reporting, and verification
43 (MRV) of carbon removal and storage is challenging. Here we provide a review of the current
44 literature showing the state-of-play of different methods for monitoring EW. We focus on geochemical
45 characterization of weathering processes at the weathering site itself, acknowledging that the final
46 storage of carbon is largely in the oceans, with potential losses occurring during transfer. There are
47 two main approaches for measuring EW, one focused on solid phase measurements, including
48 exchangeable phases, and the other on the aqueous phase. Additionally, gas phase measurements have
49 been employed to understand CO_2 fluxes, but can be dominated by short-term organic carbon cycling.
50 We stress that, although there is complexity in tracing EW CDR in the natural field environment,

51 established literature validates existing approaches, and each approach has strengths and limitations.
52 The complexity inherent in open-system CDR pathways is navigable through surplus measurement
53 strategies and well designed experiments, which we highlight are critical in the early stage of the EW
54 CDR industry.

55

56 **1 Introduction**

57 All emissions pathways which limit global average temperatures to $<2^{\circ}\text{C}$ now necessitate gigatonne
58 scale removal of atmospheric carbon dioxide (CO_2) in addition to emissions reductions (IPCC, 2022;
59 Smith et al., 2023). In order to meet national and international targets for climate change mitigation,
60 the carbon dioxide removal (CDR) industry has to scale rapidly, delivering high-quality, durable and
61 additional CDR (Campbell et al., 2022; Maesano et al., 2022; Smith et al., 2023). Projected needs for
62 durable CDR range anywhere from $0.06 \text{ GtCO}_2/\text{yr}$ to over $1 \text{ GtCO}_2/\text{yr}$ by 2030, alongside less durable
63 forestation-based methods and land management practices, which is a 30-540 fold increase from 2020
64 levels of 0.002 GtCO_2 (Smith et al., 2023). Accelerating CDR deployment within such a short time
65 frame given the financing, policy, technical and engineering challenges associated with many durable
66 CDR methods highlights the importance of rapidly validating those approaches that are available to
67 scale near-term and that can readily integrate within existing activity. Much of this validation rests on
68 scientific verification of the net atmospheric CO_2 removed, as well as the assessment of associated
69 environmental impacts. This review addresses the challenge of scientific verification by detailing the
70 current state-of-play of the multiple options for reliably quantifying and monitoring carbon fluxes
71 associated with terrestrial enhanced weathering (EW).

72

73 Enhanced weathering is considered a novel CDR technique which aims to speed up chemical
74 weathering of rocks, increasing the flux of dissolved inorganic carbon (DIC, primarily bicarbonate
75 (HCO_3^-)) to the oceans (Seifritz, 1990; Schuiling and Krijgsman, 2006; Köhler et al., 2010; Hartmann
76 et al., 2013; Taylor et al., 2016). The premise of this is that CO_2 dissolved in rain and soil waters as
77 carbonic acid is neutralized by alkaline minerals, generating stable bicarbonate ions in drainage waters
78 which, when transported to the oceans, stored in groundwater reservoirs or precipitated as carbonate
79 minerals in soils become a durable carbon store (Fig. 1).

80

81 The global riverine flux of DIC from continental weathering has regulated atmospheric CO_2 on Earth
82 over million year timescales, and currently removes $\sim 1 \text{ Gt}$ of CO_2 per year (Walker et al., 1981;
83 Berner and Berner, 2012). In order to speed up this natural process, crushed reactive rocks (e.g., basalt
84 and dunite), minerals (e.g., olivine and wollastonite) or other alkaline materials (e.g., slag, cement kiln
85 dust, or returned concrete) can be applied in agricultural settings (Renforth et al., 2015; Taylor et al.,

86 2016; Renforth, 2019; Amann et al., 2020; Haque et al., 2020; Kelland et al., 2020; Knapp and Tipper,
87 2022). Based on generalist model predictions, EW has a global CDR potential in the range of 0.5–4
88 Gt CO₂ per year (Fuss et al., 2018; Beerling et al., 2020; IPCC, 2022), which can be optimized
89 through the choice of feedstock and weathering environment (Beerling et al., 2020; Cipolla et al.,
90 2021, 2022; Baek et al., 2023; Haque et al., 2023). Such a magnitude of CDR can meaningfully
91 contribute to national and international CDR targets (Taylor et al., 2016; Beerling et al., 2020; Kantzas
92 et al., 2022; Smith et al., 2023) with water and energy requirements lower than most industrial
93 removal technologies (Eufrazio et al., 2022), no required change in land use, all while providing
94 important benefits for crops and communities (Manning and Theodoro, 2020; Swoboda et al., 2022).
95 Moreover, the infrastructure required for deployment already exists.

96

97 Enhanced weathering is an open-system CDR pathway and therefore directly monitoring weathering
98 rates, and ultimately calculating net CDR, is challenging. The complexity of this open system presents
99 a significant barrier to scaling the technology (Santos et al., 2023). Under the definition of CDR as a
100 process involving both the capture *and* durable storage of atmospheric carbon dioxide (Smith et al.,
101 2023), the capture phase refers to the formation of bicarbonate at the weathering site with storage
102 occurring primarily as dissolved bicarbonate in the ocean and long lived aquifers (Campbell et al.,
103 2022; Smith et al., 2023) or, less commonly, through the precipitation of carbonate minerals in the soil
104 (Renforth et al., 2009; Haque et al., 2020). Both storage pools are considered permanent by all current
105 carbon management definitions (pedogenic carbonates; $\sim 10^4$ years, ocean bicarbonate; $\sim 10^5$ years
106 (Berner et al., 1983; Zamanian et al., 2016; Renforth and Henderson, 2017; Kanzaki et al., 2023) but
107 differ in their CDR efficiency with a 50% stoichiometric loss of captured CO₂ occurring during
108 carbonate precipitation (see Campbell et al., 2022).

109

110 There are currently numerous approaches to estimating carbon capture at a weathering site, drawn
111 from established soil science, agronomy, geochemistry and geology literature. These approaches can
112 be broadly separated into solid, water and gas based categories. In addition, the use of soil
113 exchangeable cation concentrations presents a hybrid between solid and water based categories, but
114 would be conducted on the samples taken for solid phase analysis. Each category contains multiple
115 geochemical measurement strategies which each have scientific or operational benefits and
116 limitations, with no standard method prevailing in the field (Table 1). Given the nascent phase of EW
117 research and deployment, current crediting methodologies from standard setting bodies allow for a
118 diversity of approaches for CDR quantification (Carbon Standards International (CSI), 2022;
119 Puro.earth, 2022). This methodological framework facilitates operational research and field
120 advancement in the private sector, whilst maintaining social and environmental safeguards. Industrial
121 operations, primarily undertaken through pre-finance agreements, are largely in a research and
122 development phase with the goal of refining methodologies. In parallel, stricter protocols are being

123 developed based on the best available science which can better ensure robust credit issuance and
124 scientifically responsible operations as the industry grows.

125

126 Transport of aqueous bicarbonate through the lithosphere-hydrosphere system occurs post-capture and
127 pre-storage (Fig. 1), often associated with ‘downstream’ CO₂ losses that decrease CDR efficiency. In
128 order to make a claim for a CDR credit, downstream CO₂ losses should also be quantified as, by the
129 definition above, CDR typically refers to the CO₂ that has been both captured *and* stored. Downstream
130 losses are more difficult to monitor directly compared to capture processes. As such, Earth system
131 models and national riverine monitoring networks may show promise for addressing open system
132 losses (Calabrese et al., 2022; Kanzaki et al., 2022, 2023; Knapp and Tipper, 2022; Zhang et al., 2022;
133 Harrington et al., 2023) but there is currently little industry guidance on how to handle them in CDR
134 claims. Upstream losses (i.e. operational or embodied emissions) must also be quantified by life cycle
135 analysis (Nunes et al., 2014; Lefebvre et al., 2019; Zhang et al., 2023) and included in net-CDR
136 calculations (Carbon Standards International (CSI), 2022; Puro.earth, 2022). We further stress that full
137 assessment of additionality and robust environmental and social safeguarding policies are essential
138 components of responsible EW CDR projects. Many of these safeguards can be incorporated into
139 measurement approaches for quantifying weathering rates and carbon capture.

140

141 Carbon removal claims for EW are made based on the enhancement of inorganic carbon cycling, and
142 would typically not include any increased carbon removal by organic carbon pathways, due to the
143 major differences in permanence and durability of the different fractions (Brander et al., 2021). That
144 being said, EW feedstocks may have complex effects on different soil organic carbon fractions, as
145 addition of rock powder may stimulate mineralization of the labile carbon pool, while potentially
146 increasing the long-term stable mineral associated organic matter (Slessarev et al., 2022). As such,
147 whilst we focus on inorganic approaches here, it is important to consider wholesale carbon budgeting
148 approaches to assess the impact of EW on existing carbon management practices, such as soil organic
149 carbon (SOC) storage (Kantola et al., 2023) and wider associated ecosystem carbon removal (Goll et
150 al., 2021).

151

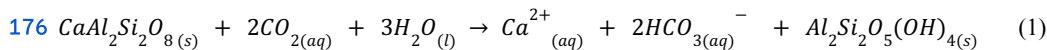
152 This review provides an orientation point for EW students, researchers, operators, regulators and
153 wider stakeholders, detailing the basis of current measurement approaches. We outline the current
154 state-of-play and summarize the strengths and limitations of different measurements for EW, primarily
155 focusing on quantification of weathering rates and captured CO₂. We consider downstream CO₂ losses
156 to be beyond the scope of this paper. This review sits alongside a broad review of experimental design
157 strategies (Almaraz et al., 2022), a recent set of thorough analytical recommendations for geochemical
158 carbon dioxide removal (Campbell et al., 2023), and a toolkit developed by CarbonPlan (Holzer et al.,
159 2023b) that outlines system wide considerations for EW.

160 2 Geochemical tracers for EW

161 2.1 Overview of the principles of EW and tracing approaches

162 In its simplest chemical formulation, EW can be considered as an acid–base neutralization reaction.
163 Carbonic acid (containing atmospheric or biogenic CO₂) is neutralized by the dissolution of an
164 alkaline material or mineral, such as a silicate mineral, producing dissolved bicarbonate, dissolved
165 silica, clay minerals and base cations (Ca²⁺, Mg²⁺, Na⁺, K⁺). This reaction converts CO₂ dissolved in
166 water to stable bicarbonate ions which are primarily durably stored as dissolved bicarbonate in the
167 ocean or, in a minority of cases, as carbonate minerals. The dissolution of most silicate minerals is
168 incongruent, meaning that mobile cations (Ca²⁺, Mg²⁺, Na⁺, K⁺) are removed via drainage waters, and
169 immobile elements (e.g., Al, Ti) either remain in the soil in recalcitrant minerals or are incorporated
170 into secondary minerals such as clays. These reactions are illustrated in Eq. 1 and 2, showing the
171 dissolution of two idealized feldspar mineral endmembers (anorthite and albite) that are common in
172 silicate rock feedstocks. In this instance, for anorthite, Ca²⁺ and bicarbonate are dissolved in waters,
173 whereas for albite, Na⁺, bicarbonate and silica are dissolved. In both cases Al and some Si remain in
174 the soil as clay minerals.

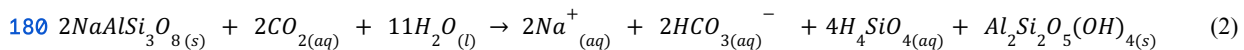
175



177 *silicate mineral (anorthite) + carbon dioxide + water → calcium + bicarbonate + clay (kaolinite)*

178

179



181 *silicate mineral (albite) + carbon dioxide + water → sodium + bicarbonate + orthosilicic acid + clay (kaolinite)*

182

183

184 A generalized silicate weathering pathway (Fig. 2) illustrates that there are two primary geochemical
185 targets for tracking weathering processes: 1) the constituents of minerals being weathered (e.g., Ca²⁺,
186 Mg²⁺, Na⁺, K⁺, Si), and 2) the carbon consumed or transformed by weathering reactions (CO₂, or
187 HCO₃⁻) (Almaraz et al., 2022; Amann and Hartmann, 2022). Of these, the former approach is a proxy
188 for mineral dissolution, allowing a calculation of weathering rates and by extension – with significant
189 assumptions – potential carbon capture. The latter provides a more direct measure, but also requires
190 assumptions on mobility and losses.

191

192 2.2 Solid phase measurements

193 2.2.1 Maximum CDR potential of rock powders

194 An estimate of the maximum CDR potential by EW can be determined using the modified Steinour
195 equation (Steinour, 1959; Renforth, 2012; Renforth, 2019). This is achieved by calculating the amount

196 of alkali and alkaline cations (wt% of CaO, MgO, Na₂O, K₂O) contained in a rock powder feedstock,
197 and then using charge balance to estimate the maximum potential for CO₂ removal (E_{pot}):

198

$$199 E_{pot} = \frac{tCO_2e}{tOre} = \frac{MW_{CO_2}}{100\%} * \left(\alpha \frac{MgO\%}{MW_{MgO}} + \beta \frac{CaO\%}{MW_{CaO}} + \theta \frac{K_2O\%}{MW_{K_2O}} + \varepsilon \frac{Na_2O\%}{MW_{Na_2O}} \right) * w \quad (3)$$

200

201 Where MW = molecular weight (g mol⁻¹), α , β , ε , θ are coefficients which account for redox speciation
202 as a function of pH (1 for pH between 3 and 10; Renforth, 2019) and w = the carbon drawdown per
203 (double-charged) cation flux to the ocean (w =1.5 to 1.7 for typical earth surface environmental
204 conditions (Renforth, 2012, 2019). Hypothetically, if the primary carbon storage pathway is through
205 carbonate mineral formation (carbon mineralization), rather than bicarbonate, then w = 1, reflecting
206 the loss of CDR potential through re-release of CO₂ upon carbonate precipitation.

207

208 Most applications of E_{pot} only focus on Ca and Mg, as the contribution of K and Na to the E_{pot} of
209 proposed feedstocks for EW is typically ~25% of that of Ca and Mg (Lewis et al., 2021). Moreover, K
210 (and to a lesser extent Na) are common constituents of chemical fertilizers which may complicate
211 cation budgeting based on field samples. The Steinhour equation can also be modified to account for
212 sulfate and phosphate in the rock powder (Renforth, 2019), sourced from salts (e.g., gypsum) pyrite or
213 apatite. In these cases, rock weathering results in cations that are charge balanced by phosphate and
214 sulfate, rather than bicarbonate.

215

216 Understanding maximum E_{pot} is important for evaluating various rock powders in order to maximize
217 CDR gains, for initial life cycle assessments (LCA) or first-order global scale models (e.g., Renforth,
218 2012; Zhang et al., 2022). Even though E_{pot} can be calculated by the cation concentration in the rock,
219 it does not account for the mineralogical composition of the rock powders, where some minerals are
220 more easily dissolved than others, nor does it account for temporal aspects of the reactions. Thus, it is
221 a single, time integrated estimate assuming fully congruent weathering of the feedstock. Its use is also
222 limited by knowledge of the internal variability of the feedstock's chemical composition. Actual CDR
223 from in situ weathering will always be smaller than E_{pot} due to the complexity of mineral weathering
224 and downstream CO₂ losses.

225

226 2.2.2 Solid-phase elemental mass balance approach

227 2.2.2a Principles

228 The loss of reactants from mineral phases can be used to calculate weathering rates, which may be
229 converted to an initial carbon capture estimate using the E_{pot} of a feedstock. Total soil + rock powder

230 mobile cation concentrations (e.g. [Ca] & [Mg]) are expected to decrease as mineral dissolution
231 proceeds and mobile cations are lost to solution (Fig. 2). The main advantage of analyzing solid
232 phases in this manner is that it creates a time-integrated signal, whereas other approaches, discussed
233 below, are heavily influenced by climatological and pedogenic parameters leading to more temporally
234 variable signals. Additionally, this approach may be integrated with current agronomic practices as
235 soil samples may be routinely taken by farmers to assess other parameters such as soil pH and cation
236 exchange capacity (CEC). Furthermore, it is possible to constrain weathering signals on a
237 field-by-field basis.

238

239 Examining total solids traces the loss of cations in the soil + rock powder to determine weathering
240 rates, but it does not track their export, so converting a rate of cation loss to CDR equivalents will be a
241 maximum estimate of carbon actually exported into the river-ocean system. Additionally, it does not
242 uniquely identify the action of carbonic acid over other potential acids in the soil, which would cause
243 an overestimate of carbon capture at the weathering site.

244

245 **2.2.2b Immobile tracers for solid phase measurements**

246 A key challenge faced by soil-based cation mass balance is that the contribution of applied rock
247 powder to cation concentrations in the soil and rock powder mixture is not certain, given
248 inhomogeneous application and mixing, sampling constraints, and potential physical erosion or
249 remobilization. This means that cation accounting based on a generalized rock powder application rate
250 for the entire field can result in an over- or under-estimation of the initial cation concentration, even
251 when samples are averaged across a field.

252

253 The problem of calculating the initial cation contribution from applied rock powder can be addressed
254 by measuring the concentration of cations in the soil relative to an immobile trace element (such as Ti,
255 Al, Th, Zr) (Reershemius et al., 2023). These principles also underlie the patent of EW operator *Eion*
256 *Corp.* (Wolf et al., 2023) who, focusing on the rare earth elements (REE) and other immobile tracers,
257 suggest that combinations of immobile tracers can be used to calculate rock powder application rates
258 (see also Kantola et al., 2023). The premise of using immobile tracers in this manner is grounded in
259 traditional sediment geochemistry in that the loss or gain of geochemical components must be
260 expressed relative to a conservative or immobile element that is not involved in the primary reaction
261 (Brimhall and Dietrich, 1987). This creates a normalization procedure that, in this case, accounts for
262 the variable mixtures of rock powder and soil at the sample point, or any erosive loss of rock powders
263 (Fig. 3). In effect, by comparing the concentrations of mobile cations to that of an immobile trace
264 element, a soil + rock powder sample can be pinned along a compositional mixing line between the
265 soil baseline and the rock powder, as shown in Fig. 3. Actual variability in rock powder application

266 and weathering activity must then be captured by ensuring a high number of samples across the entire
267 site covering representative environmental gradients.

268

269 Mass balance approaches using any immobile tracer are predicated on knowing precisely the baseline
270 soil immobile tracer (i) and cation (j) concentrations, rock powder i and j concentrations, and the
271 concentrations of i and j in the mixture after weathering. Essentially, the immobile tracer is used to
272 calculate the amount of cations added to the soil through rock powder spreading, and measurements of
273 post weathering samples of soil + rock powder mixtures inform on the remaining cation amount. The
274 difference in cation concentrations can then be expressed as a fraction of rock powder dissolved (Fd;
275 Fig. 3d) and related back to carbon capture through Eq. 3.

276

277 This approach makes two major assumptions. Firstly, the immobile tracer must be demonstrably
278 immobile in the chosen environment. Loss of some immobile tracer from the rock powder will result
279 in a conservative estimate for weathering, but if reprecipitated elsewhere in the soil column may
280 produce a mixed signal for rock powder addition in some samples and therefore distort whole-field
281 weathering estimates. Secondly, cations must be considered fully mobile and generally lost to
282 solution, and will therefore not be present in any solid soil + rock powder sample after weathering.
283 This second assumption, however, is not always applicable as cations can be (sometimes temporarily)
284 incorporated into exchangeable phases or secondary minerals (Amann et al., 2020; Fuhr et al., 2022;
285 Wood et al., 2023). Standard operating procedures for dealing with such exchangeable phases require
286 further development, with some users including pre-leaching treatments to remove them. Sieving of
287 samples to remove larger residual rock fragments and organic debris is usually practiced.

288

289 Whilst operationally scalable, one major limitation of using the solid phases for these estimates is the
290 low signal to noise ratios due to high soil cation concentrations. Hence it can be difficult to resolve
291 small differences between the soil-rock mixtures, before and after weathering. To counter this
292 problem, isotope dilution inductively-coupled plasma mass spectrometry (ID-ICP-MS) may be used
293 to improve measurement precision and be better able to resolve small changes in cation concentrations
294 (Reershemius et al., 2023). There may be cases where such high precision is not required, such as
295 where higher rock powder application rates are used, in higher intensity weathering environments, or,
296 generally, when soil and feedstock compositions are very different.

297

298 Given the requirement for a precise baseline concentration to be assumed, heterogeneity in soil trace
299 and major element composition represents an appreciable barrier to implementing solid-phase mass
300 balance approaches to tracking weathering at the field scale. This may be at least partly addressed
301 through implementing soil sampling protocols that increase the replicability of measurements (e.g.,
302 pooling, geospatial referencing). Statistical treatments of whole-field i and j concentrations of baseline

303 and post-application, post-weathering samples will likely be necessary to robustly quantify field-scale
304 compositional changes as a result of EW feedstock application and subsequent dissolution. A key
305 challenge for practitioners will be to assess the minimum sampling requirements for resolvability of
306 these signals in a range of settings, which is currently under-explored in the literature and a
307 recommended priority for ongoing research.

308

309 Lastly, the choice of immobile tracer i is an important consideration. The concentration of immobile
310 tracer in the rock powder must be significantly higher than in the soil, because: 1) this reduces the
311 requisite analytical precision for measuring a signal for rock powder addition above background
312 noise; and 2) otherwise, at low $\Delta i_{rock\ powder - soil}$, the dissolution of feedstock contributes to a stronger
313 concentration effect of i , resulting in a pronounced overestimate of rock powder addition
314 (Reershemius and Suhrhoff, 2023). This effect is true of any element i , but can be corrected easily for
315 those elements i where concentration in rock powder is several times greater than in soil (Reershemius
316 et al., 2023). Low $\Delta i_{rock\ powder - soil}$ of Th, Nb, Y, and REEs precludes these immobile tracers from being
317 used for most rock powder-soil combinations; this is also true of Ti and Al for most ultramafic rocks,
318 where Cr, Ni and Fe might be the only realistic tracers. Some proposed rock powders for EW, such as
319 wollastonite, do not contain any immobile trace elements in sufficient abundance to be used for this
320 purpose. An additional consideration for an immobile tracer i that must be tested thoroughly is the
321 extent of mobility during weathering processes in a range of settings; especially those elements, such
322 as Cr, Ni, Fe, that can also have limited mobility depending on properties such as soil redox state,
323 availability of organic colloids, and pH (Alloway, 2013). Whilst immobility might still be maintained
324 for these elements, heterogeneity in their concentrations vertically and laterally due to diagenetic
325 processes, may lead to biased results.

326

327 Kantola et al. (2023) suggest using multiple immobile trace elements in a single calculation to
328 increase the signal strength from rock powder addition in solid phase samples. This involves fitting a
329 regression to the observed concentration increase of multiple immobile trace elements and using the
330 slope of this line to calculate the rock powder application rate (Kantola et al., 2023). However, when
331 using elements that are not particularly enriched in the feedstock, this approach must account for the
332 fact that the concentration increase of multiple immobile trace elements following rock powder
333 addition to a soil is also a function of the relative concentration differences between rock powder and
334 soil for each individual element, and will be affected by feedstock dissolution (Reershemius and
335 Suhrhoff, 2023). Moreover, analytical uncertainties must be appropriately propagated to ensure
336 accuracy and significance of interpretations based on regression models. A different approach to
337 increasing the strength of a signal for rock powder addition may instead be to pin to a ratio of
338 immobile tracers, where the denominator is a tracer that is less concentrated in the rock powder than
339 in the soil (e.g. Th).

340

341 It is clear that more work is needed to develop methods to refine soil-based mass balance for
342 estimating in-field weathering rates of rock powder: primarily to improve sampling and analytical
343 practices while limiting their cost, to resolve spatial variability in estimates of field-scale weathering
344 rates, and to take into account processes such as fertilizer addition and background weathering of soil
345 constituents that may interfere with signals. Moreover, assumptions on tracer (im)mobility require
346 testing in more local environments before such methods can be robustly used for widespread CDR
347 crediting purposes.

348

349 **2.2.3 Accumulation of soil inorganic carbon**

350 With some reactive feedstocks (e.g., slag and wollastonite) or under certain climatic conditions (low
351 rainfall, high soil pH) carbonate precipitation may be favored over aqueous bicarbonate creation,
352 termed carbonation or CO₂ mineralization (Campbell et al., 2022). The CDR efficiency of the
353 mineralization pathway is half that of EW with bicarbonate formation due to CO₂ release during
354 carbonation (Fig. 2). In these cases, the formation of carbonate can be monitored as total inorganic
355 carbon (TIC). At high enough concentrations, TIC is relatively simple to quantify using calcimetry or
356 thermogravimetric analysis and, if enough carbonate is generated, can be combined with techniques
357 such as XRD analysis to characterize the carbonate mineralogy (Dudhaiya et al., 2019; Haque et al.,
358 2019, 2020, 2023; Khalidy et al., 2021). Additionally, the source of carbon and calcium can be
359 quantified using isotopic tracers (see Section 2.5; radiogenic Sr isotopes to confirm the source of Ca,
360 and stable carbon and oxygen isotopes to confirm the source of carbon) to ensure the accumulation of
361 TIC came from mineralization of silicate minerals (Knapp et al., 2023).

362

363 **2.3 Accumulation of weathering products in exchangeable phases**

364 Dietzen and Rosing (2023) suggest monitoring cation accumulation in exchangeable phases as a
365 pathway to carbon capture estimates, which may potentially be easier to resolve compared to total
366 solids approaches. In principle, this approach is based on the opposite assumption compared to solid
367 phase approaches: namely that all released mobile cations are not leaving the top soil but are retained
368 on exchangeable sites for the period in question. Exchangeable phases are geochemically reactive
369 components (clays, oxides and organic matter) within a soil that have the capacity to weakly bind
370 cations to their negatively charged surfaces. These reactions are typically considered to be rapid,
371 operating on the order of seconds to days and may include sorption and surface precipitation (Brady
372 and Weil, 2008). Often the exchangeable phases include elements bound to clays and oxides minerals,
373 but not the elements incorporated into these minerals on longer timescales due to diagenetic
374 stabilization. Elements weakly bound to organic matter can also be included, but not those directly

375 incorporated into more recalcitrant organic substances (Brady and Weil, 2008). Note that some
376 literature sources refer to 'bioavailable', 'reactive' or 'labile' pools to distinguish phases that are
377 separate to non-reactive, inert mineral phases (Bhatia et al., 2013; Larkin et al., 2021). There will be
378 overlap between such phases and the exchangeable pool, however, in reality, all of these terminologies
379 are operationally defined based on leaching protocols and are rarely exclusive in their extraction
380 (Brown, 1943; Tessier et al., 1979; Groenenberg et al., 2017; Vienne et al., 2022; Vink et al., 2022;
381 Dietzen and Rosing, 2023).

382

383 The precision of this method therefore relies on correctly timing soil sampling, and any loss of cations
384 from top soils to ground water will not be detected. Given that water (and hence the flushing of
385 cations from top soils) is a necessary condition for weathering to occur, the validity of these
386 assumptions and the temporal decoupling of weathering and cation transport can be questioned.
387 Dietzen and Rosing (2023) suggest that baseline monitoring of exchangeable and fluid phases could
388 be used to identify time periods where the loss of cations to fluids is minimal, allowing measurements
389 from the exchangeable fraction from particular seasonal points to be used for CDR estimates. But,
390 there will always be a risk of underestimating cation losses.

391

392 In some EW experiments, there is no evidence for significant cation removal by exchangeable phases
393 (Renforth et al., 2015), whilst others demonstrate quantitatively important interactions between
394 cations and secondary minerals, such as clays (Pogge von Strandmann et al., 2019, 2021; Dietzen and
395 Rosing, 2023), even up to a 100 x the concentrations seen in leachate data (Kelland et al., 2020).
396 Given the potential control of exchangeable pools onto the weathering mass balance, they may be a
397 limiting factor for identifying weathering products from solution based methods, and a suggested
398 contributor for the lack of observed weathering signals in outflow waters of field trials, particularly in
399 low pH soils (Larkin et al., 2022). Such behavior will depend on the base saturation state of the
400 exchange sites as well as soil permeability, pH, net cation exchange capacity (CEC) and surplus
401 rainfall. If there is a low CEC or high pH, base saturated soil, it will be more likely that cations are
402 transported out of the soil.

403

404 **2.4 Aqueous phases**

405 **2.4.1 Overview**

406 With a similar logic to examining exchangeable phases, accumulation of weathering products in
407 aqueous phases can also produce a wealth of information on cations and anions, including carbon
408 species (Renforth et al., 2015; Shao et al., 2015; Vienne et al., 2022; te Pas et al., 2023). In
409 experimental setups, such as columns, pots and mesocosms, the aqueous phase is often collected as a

410 'leachate'; that is a fluid that has penetrated the soil, mobilized weathering products and exited the
411 experimental setup into a collector. Infield sampling may be done via the collection of pore waters
412 through Macro Rhizon syringes, via soil lysimeters (e.g., suction cup or tension lysimeters) or even
413 shallow wells at specific depths in the soil column (see Almaraz et al., 2022). Artificial
414 cation-exchange resins in the soil have also been suggested as a method to sample waters by the
415 patent of Wolf et al., (2023) but to date, there is no published research validating this approach. Anion
416 exchange resins have also been used to measure nitrate and ammonia (Kantola et al., 2023).

417

418 Catchment or watershed scale monitoring on rivers or channels have been applied to larger scales of
419 deployment, providing integrated total system fluxes (Andrews and Taylor, 2019; Larkin et al., 2022;
420 Knapp et al., 2023). Indeed, monitoring of dissolved loads at the riverine catchment scale is the
421 primary method by which current global CO₂ removal via natural weathering is measured (Gaillardet
422 et al., 1999b; Viers et al., 2007; Hartmann et al., 2014; Moon et al., 2014; Hilton and West, 2020)
423 hinting at the scalability of this approach. It may also be possible to monitor drainage waters via
424 carefully designed artificial drainage systems (e.g., tile drains) to capture water exiting a site
425 (Andrews and Taylor, 2019).

426

427 In the field, the location, depth and timing of solution sampling will have implications for how
428 measurements will be related back to carbon capture estimates. For pore-water samples, data will
429 likely primarily reflect reactions at the weathering site including primary dissolution and secondary
430 uptake of weathering products. Water moving through a soil may be subject to additional geochemical
431 processing, such as adhesion to cation exchange sites (Pogge von Strandmann et al., 2019), that could
432 modify the EW signal. By contrast, measurements made at the catchment scale can provide total
433 system fluxes, averaging out small scale heterogeneities.

434

435 For all solution-based analysis in the field environment, challenges exist in the temporal signature of
436 aqueous phases that can vary seasonally, for example with rainfall amount and intensity that affect
437 dissolution kinetics, dilution, water flow paths through the soil, transit times and total cation export
438 (Calabrese et al., 2017; Wen et al., 2022), requiring detailed temporal consideration on sampling
439 strategies (Dietzen and Rosing, 2023) and how measurements are scaled to annual CDR estimates.
440 Additionally, particularly at large scales, it might take years for a resolvable trend to emerge (Taylor et
441 al., 2021) and so long-term monitoring, large-scale and carefully designed experiments might be
442 required, in combination with scientific guidance on sampling intervals for robust CDR estimates.

443

444 Solution based analysis requires assessment of water flow in order to convert concentrations into a
445 flux (the total amount of inorganic carbon exiting to catchment waters per year) and ultimately
446 calculate the mass of carbon exiting the system. Typically there is a measurement resolution mismatch

447 between how often a discharge measurement is taken or modeled (resolution of minutes to daily) and
448 how often a concentration measurement is made (at least biweekly, sometimes monthly). Therefore, a
449 load estimation method is required to calculate an annual flux (e.g. Moatar and Meybeck, 2005).
450 Chosen load estimation methods require some assumptions to be made about concentration behavior
451 in between sampling points. Measurement of discharge at the watershed scale may be more
452 straightforward with the proper installation and calibration of a gauging station. At the smaller field
453 scale, modeling or calculation of predicted flow based on measured climatic parameters (via an onsite
454 weather station) and physical soil properties can be used to estimate discharge (Alley, 1984; McCabe
455 and Markstrom, 2007).

456

457 **2.4.2 Base cations and dissolved silicon**

458 The base cations (Ca^{2+} , Mg^{2+} , Na^+ and K^+) are mobile, and form the main dissolved cations in natural
459 waters. Potassium (K^+) and (Ca^{2+}) are more likely to be uptaken by plants, with potassium being a key
460 nutrient. Sodium (Na^+) and potassium (K^+), are more likely to remain in the aqueous phase, but are
461 limited by their availability in CDR rock powders and have a lower CDR potential per mass due to
462 forming singly charged cations. Ca^{2+} and Mg^{2+} are more abundant in CDR rock powders but are more
463 likely to adhere to the exchangeable sites (Whitworth, 1998; Bergaya et al., 2006; Dietzen and
464 Rosing, 2023), and Ca^{2+} will form pedogenic carbonates in some EW operations (Haque et al., 2020;
465 Khalidy et al., 2021). Numerous studies suggest that Mg^{2+} is the most suitable cation for estimating
466 weathering rates in the exchangeable fraction and plays a larger role in potential CO_2 uptake (Renforth
467 et al., 2015; Pogge von Strandmann et al., 2021; Dietzen and Rosing, 2023). Moreover, given that
468 Mg^{2+} is not as readily incorporated into carbonate minerals or uptaken by plants compared to Ca^{2+} , it
469 may be easier to trace in solutions.

470

471 Similarly, Si will be a major component of many EW feedstocks and its presence in solution could
472 directly indicate weathering activity. It is more difficult, however, to relate Si concentrations back to
473 carbon capture given the mineral partitioning of Si within the feedstock. For example, the presence of
474 Si in non-alkaline silicate minerals (including amorphous phases) could supply Si without cations.
475 Silicon can also be removed from solution to form secondary minerals (e.g. Kelland et al., 2020). It
476 has furthermore been suggested that silica saturation may limit feedstock dissolution and the CDR
477 potential of EW (Köhler et al., 2010; Hartmann et al., 2013; Harrington et al., 2023), however the role
478 of silica saturation in limiting enhanced weathering is debated (Schuiling et al., 2011).

479 **2.4.3 Anions**

480

481 In natural waters at neutral range pH, the dominant dissolved anions are sulfate, nitrate, chloride and
482 bicarbonate. Minor contributions from phosphate and borate may be present in some waters. The sum
483 of major anions (Cl^- , SO_4^{2-} , NO_3^- , HCO_3^-) minus the sum of major cations (Ca^{2+} , Mg^{2+} , Na^+ and K^+) in
484 equivalents is equal to zero due to the law of electroneutrality. The normalized inorganic charge
485 balance (NCIB = $(\Sigma^+ - \Sigma^-)/(\Sigma^+ + \Sigma^-)$ in %, where Σ^+ is the sum of cations and Σ^- is the sum of
486 anions, in equivalents) or charge balance error (CBE) is a key indicator of water data quality, with
487 values typically greater than $\pm 5\%$ for high quality measurements, and should always be within $\pm 10\%$
488 (Fritz, 1994).

489

490 Measurement of anions are required to understand not only the quality of the measurement but also to
491 understand the acidity source (carbonic acid vs. strong acids; see section 3.2), and to correct cation
492 measurements for rainwater inputs (cyclic salts) and dissolution of evaporites (such as gypsum that is
493 commonly used as an agricultural amendment). Bicarbonate concentrations in neutral range pH waters
494 may be calculated using major anion and cation measurements via charge balance, assuming that all
495 remaining positive charge after subtracting Cl^- , SO_4^{2-} , NO_3^- (in equivalents) is charge balanced by
496 HCO_3^- (e.g., Galy and France-Lanord, 1999).

497

498 2.4.4 Total alkalinity (TA), pH and DIC

499

500 Dissolved inorganic carbon (DIC) is a term used to encompass all inorganic carbon species in a liquid,
501 including CO_2 , carbonate, bicarbonate and carbonic acid. Thus, it can give the most direct
502 measurement of bicarbonate release from mineral weathering (Amann et al., 2020; Almaraz et al.,
503 2022). DIC measurements can be performed with several types of equipment that require minimal
504 technical skills (e.g., coulometry). For soil pore waters, the main issue is that the partial pressure of
505 CO_2 ($p\text{CO}_2$) is much higher than atmospheric $p\text{CO}_2$ due to respiration. Thus, samples need to be
506 hermetically saved (and with minimum headspace), from the moment they are collected in the field
507 until they are analyzed, to avoid degassing of molecular CO_2 (Reiman and Xu, 2019). Special care
508 needs to be taken for samples at lower pH values in which the concentration of dissolved molecular
509 CO_2 is higher. In other cases, samples can be left open to the air to equilibrate with atmospheric CO_2 ,
510 after which DIC can be measured a second time, simulating equilibration which would have happened
511 when the soil pore-waters enter a watershed.

512

513 In neutral pH waters, DIC can be approximated by total alkalinity (TA) measurements. This is only
514 true, however, if the only proton (H^+) receptors (the bases) are largely from hydroxide (OH^-),
515 bicarbonate (HCO_3^-) and carbonate (CO_3^{2-}), and pH is between 6.3 and 10.3 (see Bjerrum plot, Fig. 5).
516 More strictly, TA refers to the milliequivalents (mEq) of H^+ used while titrating a water sample with

517 an acid of known concentration, usually via Gran Titration (Gran, 1952; Stumm and Morgan, 1996;
518 Wolf-Gladrow et al., 2007). Thus, the measured TA is an approximation for DIC, which in most
519 natural freshwaters is bicarbonate, and hence can be used to estimate CDR. Any two of alkalinity, pH,
520 $p\text{CO}_2$ and DIC can be used to calculate bicarbonate concentrations in waters. These calculations can
521 be performed in PHREEQC (Parkhurst, 1995).

522

523 The advantage of TA is that it is a simple measurement to make with no specialist equipment needed,
524 and is routinely measured during watershed monitoring by, for example, governmental bodies
525 (Hartmann et al., 2014; USGS, 2019). Total alkalinity is a conventional parameter used to calculate
526 the bicarbonate concentration of natural freshwaters at circum-neutral pH (Andrews et al., 2016;
527 Amann and Hartmann, 2022; Holzer et al., 2023a; Knapp et al., 2023). Caution should be maintained,
528 however, as TA can be affected by the presence of other accepting bases in addition to DIC. For
529 example, in waters with high dissolved organic carbon (DOC), total alkalinity might be a poor
530 approximation for bicarbonate concentrations (Wolf-Gladrow et al., 2007; Kerr et al., 2021).

531

532 2.4.5 Electrical conductivity (EC)

533 Electrical conductivity (EC) reflects the total ion concentration of a solution and hence can proxy the
534 accumulation of weathering products, offering a potentially more scalable solution to CDR
535 monitoring. The benefit is that EC can potentially be monitored in real time using sensors, whilst TA
536 requires ex-situ lab analysis. Amman & Hartmann (2022) identified consistent correlations between
537 TA and EC, thought to reflect the covariation of TA and cation concentrations. This potentially means
538 EC could be used in specific situations, coupled with pH measurements, where assumptions about TA
539 and DIC speciation can be made and bicarbonate concentrations can be calculated successfully using
540 speciation modeling software such as PHREEQC (Parkhurst, 1995). Robust and representative
541 calibration datasets should be used to validate and monitor the use of EC in field environments as the
542 relationship of EC to TA will vary with different ionic compositions.

543

544 2.5 Isotopes

545 2.5.1 Overview

546 Measuring isotope compositions is more expensive than most of the MRV approaches introduced thus
547 far, and requires more specialist infrastructure, thus they are less likely to be an integral part of routine
548 MRV approaches. However, isotope-based approaches can yield additional important information that
549 is complementary to other methods and provide a fuller picture of the EW process. In particular, they

550 can play a fundamental role in determining some of the underlying processes and in calibrating
551 reactive transport models.

552

553 The approaches in the previous sections all have in common that they assess the absolute
554 concentrations of certain elements or ions. While it is essential to assess elemental reservoirs and
555 fluxes, isotope ratios can yield additional information such as the nature of the sources and sinks of
556 elemental fluxes, or processes that modulate these fluxes (Faure and Mensing, 2005). For example,
557 stable isotope systems are often used to infer mixing of different element sources, as different sources
558 can have very different isotope signatures. They are also used to infer processes such as the formation
559 of secondary phases or cation sorption onto exchangeable sites because some isotopes are easier to
560 exchange, for example as a result of higher or lower mass (i.e., they fractionate them).

561

562 Radiogenic isotope systems are typically used to trace sources rather than processes. As a result, for
563 traditional radiogenic isotope ratios, sample composition typically depends on the isotope
564 composition of the source mineralogical phases. Complexity in interpretation arises, however, because
565 isotope ratios are usually modified by secondary controls, such as biological (e.g. respiration),
566 environmental (e.g. temperature) or procedural (e.g. laboratory separation and measurement)
567 processes.

568 **2.5.2 Stable carbon and oxygen isotopes**

569 Stable carbon and oxygen isotopes ($\delta^{13}\text{C}$ and $\delta^{18}\text{O}$) are relatively simple to measure and can inform on
570 the source of C in soil fluids and carbonates. If the $\delta^{13}\text{C}$ of each carbon source is distinct and known,
571 then measured $\delta^{13}\text{C}$ of water outflows could inform on the relative proportion of each source
572 (Manning et al., 2013). For example, CO_2 in soil waters is typically derived from organic respiration,
573 giving it a low $\delta^{13}\text{C}$ value (-27 to -12.5‰; Vogel, 1993), whereas carbonate rocks and carbonate
574 amendments ('AgLime'), derived from marine carbonate deposits, have higher, and distinct, $\delta^{13}\text{C}$
575 values. Potentially $\delta^{13}\text{C}$, coupled with $\delta^{18}\text{O}$, can help separate sources of C and identify contributions
576 from silicate weathering vs. carbonate weathering in fluids as well as pedogenic and lithogenic
577 carbonates in soils (Cerling, 1984; Schulte et al., 2011). To date, $\delta^{13}\text{C}$ and $\delta^{18}\text{O}$ have been used to
578 partition sources in carbonates at enhanced weathering sites (Knapp et al., 2023).

579 **2.5.3 Radiocarbon**

580 Radiocarbon (^{14}C -dating) is expensive to analyze and requires both specialist preparation of samples,
581 and equipment for measurement (e.g., accelerator mass spectrometry). However, radiocarbon can
582 provide valuable insights into the age of products derived from enhanced weathering, and can help to
583 pin-point modern atmospheric carbon sources with lower uncertainty than traditional stable carbon
584 and oxygen isotopes (Knapp et al., 2023). Radiocarbon may be incorporated into the products of

585 enhanced weathering, such as carbonates, derived from atmospheric CO₂ which currently has a fixed
586 ¹⁴C content from cosmic production in the atmosphere. Once incorporated, ¹⁴C starts to decay and the
587 age of the carbonate since formation can be measured. Older sources of carbon (>~60 kyrs), such as
588 bedrock carbonate and shales, have isotopically ‘dead’ C, where ¹⁴C has fully decayed, potentially
589 helping separate carbon supplied by EW from other sources of C in the system. Coupled with total
590 carbon content, it is possible to extract a rate of atmospheric C removal using this technique (Knapp et
591 al., 2023). Nevertheless, caution should be exercised when using both radiocarbon and stable carbon
592 isotopes as these methods are affected by CO₂ exchange and kinetic fractionation that may lead to
593 misleading interpretations (Stubbs et al., 2023).

594

595 **2.5.4 Radiogenic strontium**

596 Radiogenic strontium (Sr) isotopes (⁸⁷Sr/⁸⁶Sr) are a common tracer for natural weathering reactions
597 and sources of weathering fluxes (Blum and Erel, 2003; Faure and Mensing, 2005). Radiogenic Sr
598 (⁸⁷Sr) is produced from ⁸⁷Rb through radioactive (β-) decay; hence the name radiogenic. Radiogenic
599 Sr is usually normalized to non-radiogenic, stable ⁸⁶Sr to facilitate comparison between phases with
600 different Sr concentrations (Blum, 1995; Blum & Erel, 1995, 2003). Silicate rock ⁸⁷Sr/⁸⁶Sr differ
601 according to rock type (mantle or crustal, as Rb and Sr are fractionated during partial melting, with Rb
602 concentrated in the melt) and age (Blum and Erel, 2003; Faure and Mensing, 2005). Carbonates and
603 evaporites can inherit ⁸⁷Sr/⁸⁶Sr values from the ocean in which they are deposited, and have values
604 which are distinct, and typically lower, than silicates. As a result, different rock types have distinct
605 isotope compositions that can be used to trace the dissolution of silicate feedstocks in EW.

606

607 Strontium cations are relatively mobile, and Sr readily substitutes for Ca in minerals as they have
608 similar atomic radii. Strontium enters pore waters and streams on a similar timescale as major cations,
609 and therefore can be used to trace cation sources, in particular Ca. Hence, the isotope composition of
610 Sr in effluent water can be used to investigate what mineralogical phases contribute to the dissolved
611 signals through their dissolution (Larkin et al., 2022). If the Sr isotope composition of soils and
612 feedstocks, as well as Sr concentrations of the feedstock, are known, this can be used to estimate
613 lithology-specific weathering rates at catchment scales (Négrel et al., 1993; Gaillardet et al., 1999a;
614 Suhrhoff et al., 2022). This approach has also been applied to EW and used to estimate the relative
615 cation flux contribution of carbonate and silicate weathering, and hence calculate CDR using cation
616 stoichiometry (Larkin et al., 2022). Caution should be applied when using radiogenic Sr if EW
617 feedstocks contain carbonates, as carbonates dissolve much quicker than silicate minerals and even
618 trace amounts of carbonates are sufficient to dominate Sr isotope signatures of weathering fluxes,
619 particularly in early weathering stages (Harris et al., 1998; Aubert et al., 2001; Jacobson et al., 2002).

620 2.5.5 Novel isotope tracers

621 Novel isotope tracers, such as magnesium (Mg), lithium (Li), silicon (Si), and stable strontium (Sr)
622 can be used to trace processes such as secondary mineral formation. The majority of work to date on
623 these isotope systems has revolved around quantifying fractionation factors and natural element
624 cycling (Penniston-Dorland et al., 2017; Teng et al., 2017), but EW-specific applications are
625 increasing (Pogge von Strandmann et al., 2021; Vienne et al., 2023). For these isotopic tracers strong
626 fractionations are induced by interactions with secondary minerals, thus potentially allowing
627 quantification of secondary mineral formation using isotope mass balance, that could inform on cation
628 loss to exchangeable phases, or potential re-release of CO₂ during secondary mineral formation (see
629 section 3.3; Campbell et al., 2022). The initial isotope signature of different feedstocks might also be
630 sufficiently unique to use as a source tracing tool, similar to radiogenic Sr.

631 2.6 Gaseous phase

632 Less research is available on the use of gas phase measurement for tracing EW in agricultural settings,
633 which has been demonstrated in mine waste EW applications (e.g., Stubbs et al., 2022). However, in
634 principle, changes in soil *p*CO₂ and soil CO₂ efflux could be used to calculate CDR. Carbon dioxide
635 removal by EW could potentially lead to a measurable decrease in the CO₂ efflux at the soil surface.
636 Resolution of the EW signal is, however, unlikely in most cases as CO₂ fluxes from organic cycling
637 tend to be an order of magnitude higher than inorganic (Weil and Brady, 2017). Gas measurements
638 could further be expanded to include other GHG fluxes like CH₄ and N₂O, which can also be
639 influenced by rock powder application (Chiaravalloti et al., 2023).

640

641 Varying interpretations about the effects of rock powders on gas fluxes have been obtained to date
642 using gas flux chambers. Dietzen et al. (2018) found no significant increase for cumulative CO₂
643 emissions for high rates of olivine application in an incubation experiment with organic rich acidic
644 topsoil (0-10 cm), although corresponding lime application increased CO₂ by 221%. In a similar
645 experiment, Yan et al. (2023) found significantly increased CO₂ emissions due to soil organic carbon
646 mineralization when mixing 12 different soil types with wollastonite (although wollastonite
647 application is extremely high at 10 wt%). Vienne et al. (2023) found significantly reduced CO₂
648 emissions in a mesocosm experiment with high (100 t ha⁻¹) basalt application rates compared to their
649 control, although the addition of earthworms to the basalt plots increased the emission. Preliminary
650 results of automated CO₂ measurements point towards more significant and consistent data than for all
651 other phases (plant, soil, water), but identify an overall increase in CO₂ efflux from soils (Paessler et
652 al., 2023). Gas measurements with the flux chamber LI-COR system confirm the CO₂ drawdown
653 potential of ultramafic rocks and oxides (Rausis et al., 2022; Stubbs et al., 2022), although these
654 experiments were conducted without soil.

655

656 Despite being important contributions to the nascent field of gas phase measurements, a major
657 limitation of the flux chamber approach (Vienne et al., 2023) is that those are point measurements of
658 the highly variable daily CO₂ flux curve. The extrapolations of these point measurements might result
659 in significantly different results depending on the spatio-temporal pattern with which measurements
660 have been taken. Automated flux chamber experiments (Paessler et al., 2023) can partly overcome the
661 temporal resolution problem but are not a scalable solution. Besides the importance of feedstock
662 mineralogy, these studies found the major parameters influencing CO₂ drawdown efficiency to be
663 water content, porosity, and permeability. Large scale measurements have been employed through
664 eddy covariance towers (Kantola et al., 2023). These measurement towers yield valuable data about
665 overall ecosystem carbon dynamics. However, the sensor height of somewhere between 1 to 2.5 m
666 might cause significant dilution of the gas phase through the overlay of various fluxes, and thus not
667 provide the necessary resolution needed for in-depth discrimination of driving mechanisms.

668

669 **3 Sources of uncertainties in CDR estimates**

670 **3.1 Multidimensionality and sampling strategies**

671 A comprehensive measurement strategy will capture variability in CDR estimates incorporating
672 natural infield spatial and temporal variability, systematic uncertainty from measurement approaches,
673 and analytical external reproducibility. We expect a multidimensional approach would create a pool of
674 CDR estimates and would allow for a data distribution to be generated. Such an intercomparison
675 would also allow for internal consistency checks and quality control on all data generated, including
676 identification and investigation of any outliers. The most conservative estimate of CDR would be to
677 utilize the lowermost capture estimates, as this corresponds to a high probability of removal.
678 However, combining different measurement methods and spatial scales would allow for statistical
679 treatment of all datasets and a distribution to be produced, resulting in an overall CDR estimate with
680 appropriate confidence intervals. Uncertainty could then translate into carbon removal credit
681 discounting, similar to suggestions from *Frontier* based on Verification Confidence Levels (Klitzke et
682 al., 2022). Understanding any systematic biases and assumptions, due to different measurement
683 approaches, will be paramount to produce the most accurate and precise CDR value. In addition to
684 this, measurement and accurate quantification of the baseline and counterfactual scenario, which will
685 need to be dynamic and measured via suitable controlled trials, has to be taken into consideration in
686 the overall measurement. Understanding and appropriate consideration of statistical significance,
687 heterogeneity and error propagation are central to proper interpretation of any data generated.
688 Compounded with uncertainties from measurement approaches, all methods are limited by the ability

689 to produce data that is representative of the EW activity area. Currently, there is no guidance from
690 standard bodies for how to handle representative sampling specific to EW (Campbell et al., 2023).

691

692 Additional uncertainties may derive from the estimates of rock powder application rate. The
693 logistically simplest method to estimate application rates is via spreading operation data.
694 Alternatively, there is potential for using immobile trace elements in pre- and post- application soils to
695 either estimate true applications rates, or use as a normalization procedure to account for application
696 rate variance (Kantola et al., 2023; Reershemius et al., 2023; Wolf et al., 2023). These solid phase
697 approaches, however, rely on accurate extrapolation across a deployment area. Importantly, high
698 application rates (50–100 t ha⁻¹) that exceed practical agronomic application rates (1–20 t /ha⁻¹,
699 Swoboda et al., 2022) are typical for most ongoing EW experiments in order to obtain clear signals.
700 However, such large amounts, especially when surface applied or mixed only in a shallow (0–10 cm)
701 soil layer, might introduce alkalinity hotspots upon dissolution and thereby significantly alter the
702 micro- and macropore saturation states, which could in turn slow dissolution kinetics. Thus,
703 extrapolating CO₂ drawdown rates from such high application amounts might be prone to error.

704

705 Temporal uncertainty is perhaps one of the largest limiting factors for EW measurement approaches.
706 The weathering of silicate minerals is a continuum, meaning that the removal of CO₂ on site follows a
707 weathering curve which may continue on decadal to centennial timescales (Kanzaki et al., 2022).
708 Each method outlined here is applicable to certain time windows, with only solid phase measurements
709 providing a temporally integrated weathering measure. In addition to this, there is spatial and temporal
710 overlap between mineral dissolution, transport and storage (Fig. 1). While beyond the scope of this
711 review, we call for clear guidance from regulators as to what point in time a credit can be issued
712 relative to measurement taken at the weathering site.

713 **3.2 Non-carbonic acids**

714 The long term use of chemical, nitrogen and phosphorus based fertilizers in nutrient poor soils may
715 lead to complications for tracing enhanced weathering as well as reducing the CDR efficiency
716 (Andrews and Taylor, 2019). Application of certain fertilizers may lead to the formation of strong
717 mineral acids, including nitric and phosphoric acid. Sulfuric acid can also be present if feedstocks,
718 such as some ultramafic rock types, contain sulfide minerals (Lerman and Wu, 2006; Horan et al.,
719 2019; Relph et al., 2021). Non-carbonic acids present multiple complications for CDR estimates
720 (Taylor et al., 2021; Zhang et al., 2022). Firstly, they are much stronger than carbonic acids, and hence
721 readily provide acidity for mineral dissolution. This means that alkaline silicate minerals can be
722 dissolved by non-carbonic acids, releasing cations (red-dashed arrow, Fig. 2), but with no CO₂
723 sequestration (no HCO₃⁻ formation), effectively decreasing the CDR potential for the rock powder.

724 That said, the export of cations from the weathering site could help buffer downstream processes and
725 CO₂ loss.

726

727 As a result of unknown acid dissolutions, any CDR method that measures only cation concentrations
728 as a weathering product (such as soil only approaches) cannot distinguish which acid caused
729 weathering and hence the true amount of CO₂ removed. For liquid based approaches, however, it may
730 be possible to use the relationship of HCO₃⁻ vs. [Ca²⁺ + Mg²⁺] as evidence for carbonic acid
731 weathering (after correcting for rainfall and fertilizer salts; Hamilton et al., 2007; Perrin et al., 2008;
732 Larkin et al., 2022). Non-carbonic acid weathering supplies cations without HCO₃⁻, creating
733 anomalous bicarbonate-cation relationships. Furthermore, water NO₃⁻ concentrations could be used to
734 estimate the degree of onsite/in situ strong acid weathering and correct for cation supply by strong
735 acids, helping refine CDR estimates in the case of fertilizer use (Larkin et al., 2022). A recent study
736 on EW with basalt powders in the midwest USA identified that less than 2% of the total cation flux
737 was derived from nitric acids (Kantola et al., 2023), hinting that such losses may be minor. But this
738 must be characterized for more environments. Moreover, nitrate, as a key nutrient, is short-lived in
739 most natural environments (Meybeck, 1982) and so the long term fate of weathering products from
740 nitric acid weathering is not known. Dietzen and Rosing (2023) suggest that the contribution of
741 non-carbonic acids to soil pH can be accounted for using the difference between pH predicted by
742 pCO₂ alone and the true pH of the soil, potentially deriving a correction factor for mineral weathering
743 due to non-carbonic acids. Importantly, their approach suggests that, depending on soil pCO₂, below
744 pH 4.5-5.5, more than 50% of weathering occurs due to strong acids. Only above a pH of 5.2-6
745 (again, depending on soil pCO₂) can most of the weathering be assumed to derive from carbonic acid.
746 Clearly, in such settings, accurate quantification of strong acid weathering is of prime importance for
747 overall carbon budgets.

748

749 Even if estimates of non-carbonic acid weathering can be made, high baseline weathering rates,
750 caused by extensive historical fertilizer use, can decrease the signal–baseline ratio making it difficult
751 to resolve weathering changes as a result of EW activity (Larkin et al., 2022). Cation interactions with
752 fertilizer components can add further complications to measuring protocols, for example the
753 formation of hydroxyapatite minerals (Wood et al., 2023) that remove cations from solution but are
754 robust enough to avoid extraction via leaching methods.

755

756 Similar to the ongoing literature discussions of Ag-lime as a source or sink of CO₂, in the case where
757 soil (pedogenic) carbonates are a significant storage pool, strong acids present a risk of reversal
758 (storage failure) through carbonate dissolution. CO₂ emission is also applicable if the EW material
759 itself contains any carbonate minerals, e.g., in concrete, or trace calcite in mafic rocks (Dietzen et al.,
760 2018; Kemp et al., 2022; Larkin et al., 2022; Zhang et al., 2022). Ag-lime, as well as silicate minerals,

761 may also potentially help offset excess acidity from non-carbonic acids, allowing further weathering
762 by carbonate or silicate minerals to be via carbonic acid instead (Hamilton et al., 2007).

763

764 3.3 Authigenic clay formation

765 With the supply of silica, aluminum, iron and cations from rock powder dissolution, the formation of
766 secondary minerals is naturally enhanced. In addition to carbonate minerals, the most common
767 secondary minerals are authigenic clays, amorphous silica, metal oxides and oxyhydroxides. Their
768 formation is a function of weathering congruence, a term that describes the tendency for a mineral to
769 dissolve completely and for the weathering products to be removed in solution, and is controlled by
770 factors such as dissolution kinetics, ambient conditions (pH, eH), rainfall and especially porosity and
771 permeability. Secondary minerals can form coatings on primary minerals, thereby isolating the
772 mineral surface from reactive fluids and decreasing weathering rates, but the impact on dissolution
773 rates is highly contextual (see Oelkers et al., 2019 for review).

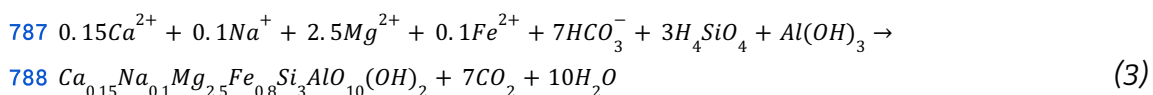
774

775 By extension, it is not clear if CDR and its rate linearly increase with feedstock application, or
776 whether high feedstock application rates promote supersaturation of secondary phases and surface
777 passivation, which may act as a negative feedback on the CDR rate. Potentially, secondary mineral
778 formation could increase reaction kinetics in some cases as high elemental saturation states may limit
779 primary mineral dissolution (Köhler et al., 2010; Schuiling et al., 2011). Secondary precipitates can
780 thereby decrease the fluid saturation state and potentially promote primary mineral dissolution
781 (Harrington et al., 2023). From a monitoring perspective, secondary minerals increase the cation
782 exchange capacity of the soil, which has implications for identifying weathering signals using liquids.

783

784 One further complication deriving from authigenic clay mineral formation (“reverse weathering”) is
785 the potential for CO₂ degassing (Fuhr et al., 2022) e.g.:

786



789

790 In marine settings, the importance of reverse weathering, and increased CO₂ flux, is clear for global
791 carbon cycling on geological time scales (Isson and Planavsky, 2018; Bayon et al., 2022). That said,
792 the role of reserve weathering in terrestrial soils and EW applications is poorly understood (Renforth
793 and Campbell, 2021).

794 **3.4 Vegetation**

795 Vegetation represents an immediate complication for CDR estimates based on liquids and
796 exchangeable phase analysis, as they will selectively remove weathering products from solution.
797 Thus, in order to complete the weathering mass balance, vegetation must be sampled to estimate
798 cation loss from the system (Shao et al., 2015; Reershemius et al., 2023). Without accounting for this
799 cation loss, there is a risk of underestimating the cation released by rock powder dissolution. That
800 said, the effects are dependant on the cation species, and plant uptake has been shown to be relatively
801 minor in comparison to cation release from basalt powder by weathering in EW field trials with
802 corn/soy and miscanthus in the US Midwest (Kantola et al., 2023). Monitoring vegetation chemistry is
803 also important for understanding the health risk of metals sourced from rock powders (Dupla et al.,
804 2023), and must follow standardized agronomy practices that consider metal compartmentalization in
805 plants and decrease exposure risk (Brune et al., 1995; Thomas and Reid, 2021). One of the biggest
806 limitations caused by vegetation is simply the removal of liquids from the soil, which makes in-field
807 liquids sampling difficult and contributes to uncertainty in flow rate calculations.

808

809 The impacts of cation removal by vegetation on wider system carbon cycling is currently
810 understudied. For example, the vegetative removal of cations will disturb the charge balance of
811 anions, including bicarbonate, in remaining pore waters (Britto and Kronzucker, 2008; Amann et al.,
812 2022). The spatial and temporal aspects must also be considered, as, similar to organic carbon cycling,
813 cation cycling in vegetation will be short term with the potential to return cations to the weathering
814 system (Banwart et al., 2009).

815

816 **4 Discussion and Conclusion**

817 While EW is a relatively new approach to CDR, the underlying science behind quantifying
818 weathering rates in soils is well established and EW specific research is progressing rapidly.
819 Moreover, while quantification of both weathering and subsequent carbonation rates should be
820 advanced further through research, multiple methods exist today that are readily available to form the
821 foundation of MRV approaches, primarily through tracking mineral constituents or directly
822 monitoring bicarbonate formation and export. The majority of measurement types can be made in
823 different settings, including experiments that explore weathering fundamentals and dissolution
824 kinetics, or field settings that monitor real world processes. This allows for a detailed determination of
825 weathering parameters through the combination of several measurement types, and a more robust
826 estimate of atmospheric CO₂ removal. The efficacy of each approach in EW operations will vary with
827 application material, soil conditions and soil management strategies that dictate the level of
828 complexity of the system.

829

830 Considering the future scaling of the EW industry to reach the projected gigatonne removal potential,
831 robust measurement campaigns can provide the foundation for geochemical modeling, including EW
832 specific reactive transport models (Kelland et al., 2020; Kanzaki et al., 2022; Vienne et al., 2022).
833 However, a strong measurement component is urgently required to refine, calibrate and validate
834 geochemical models. This is particularly relevant as current favored reaction transport or simplified
835 dissolution models are described as more comparable to closed system batch reactors than natural
836 field conditions, lacking real world processes such as wetting-drying cycles, spatial resolution of
837 permeability and flow paths, secondary mineral formation (Kelland et al., 2020) or exchange
838 processes (Beerling et al., 2020; Kantzas et al., 2022). Moreover, there is large uncertainty in core
839 input parameters such as mineral dissolution kinetics (Calabrese et al., 2022) and models calibrated
840 under certain experimental setups fail to predict empirical datasets in other applications (Vienne et al.,
841 2022). The EW community would benefit from an intermodel comparison project, similar to those
842 used for climate models (CMIP), especially when considering downstream processes.

843

844 The success of EW as a CDR pathway will vary based on localized factors (e.g., climatic, geologic
845 and agricultural; Cipolla et al., 2021, 2022), analogous to controls on natural weathering rates (West et
846 al., 2005; Brantley et al., 2023), as well as rock type (mineralogy, particle size and surface area;
847 Taylor et al., 2016; Renforth, 2019). Whilst rock powder dissolution in soil environments is highly
848 complex at a local scale, leading to high spatial variability in measurements, this variability will
849 become averaged out at larger spatial scales. As EW operations in a given catchment area expand,
850 riverine monitoring may become the primary approach for quantification of carbon removed,
851 rendering measurements at the soil level of secondary importance. To successfully identify enhanced
852 weathering signals in rivers, however, requires that the signal is resolvable over baseline variability,
853 which is challenging in environments of high baseline weathering activity, for example due to historic
854 fertilizer use (Larkin et al., 2022; Mu et al., 2023). Innovative approaches to monitoring over larger
855 spatial and temporal scales should be explored, as they may be required to complement local
856 measurements and models for deployment at scales of megatonne or gigatonne CDR across wider
857 geographies.

858

859 All measurement approaches require an accurate dynamic baseline via controlled trials (e.g.,
860 'untreated' measurements) to quantify counterfactual weathering rates, that is, carbon capture that
861 would have happened in the absence of application of EW feedstocks. This is particularly important to
862 understand if feedstocks are replacing other agricultural amendments (such as Ag-lime or synthetic
863 fertilizers) or in scenarios where rock powder application might already be practiced (albeit at lower
864 application rates than are typical for EW; Swoboda et al., 2022). It is important that the baseline
865 operations cover highly comparable geographic and climatic gradients as active EW applications.

866

867 At this point in time, all EW operations, private sector or academic, are in a phase where data
868 production is paramount to collectively solve the challenges of quantifying weathering activity. Given
869 the complexity of the soil system, and potential for competing processes to create uncertainty, we
870 stress that multidimensional measurement campaigns should be undertaken and prioritized.
871 Ultimately, scaling of EW will depend on public acceptance of this CDR approach; it is therefore in
872 the interest of all stakeholders to be transparent in their measurement approaches and to provide a
873 scientific basis and rationale for deployment of EW as a solution to address climate change.

874

875 **Acknowledgements**

876 JSC was funded by the European Union's Horizon 2020 Research and Innovation Program under
877 grant 869357 (project OceanNETs: Ocean-based Negative Emission Technologies—analyzing the
878 feasibility, risks, and co-benefits of ocean-based negative emission technologies for stabilizing the
879 climate). TJS is funded by the Swiss National Science Foundation (grant P500PN_210790). CNM is
880 funded through the Grantham Foundation for the Protection of the Environment.

881

882 M. O. Clarkson, C. S. Larkin and P. Swoboda declare that they work for a for-profit company
883 (InPlanet GmbH) deploying enhanced weathering for carbon dioxide removal. J. Campbell sits on the
884 science advisory board for InPlanet.

885

886 **Author contributions**

887 MOC instigated the article, and wrote the first draft. CSL, TJC, TR, CNM and TJS all contributed and
888 wrote sections, with all authors contributing to the final version. All authors approved the submitted
889 version.

890

891 We acknowledge and thank Elisabeta Pedorosa for early discussions on some of the material in the
892 manuscript

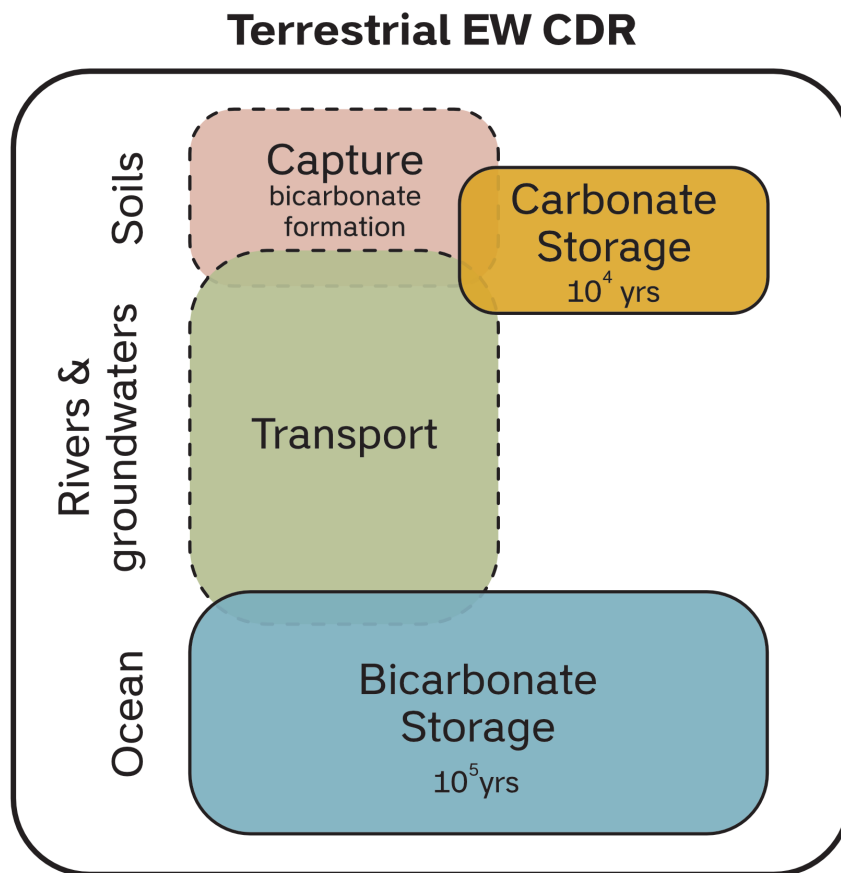
893

894

895 **Figures**

896

897

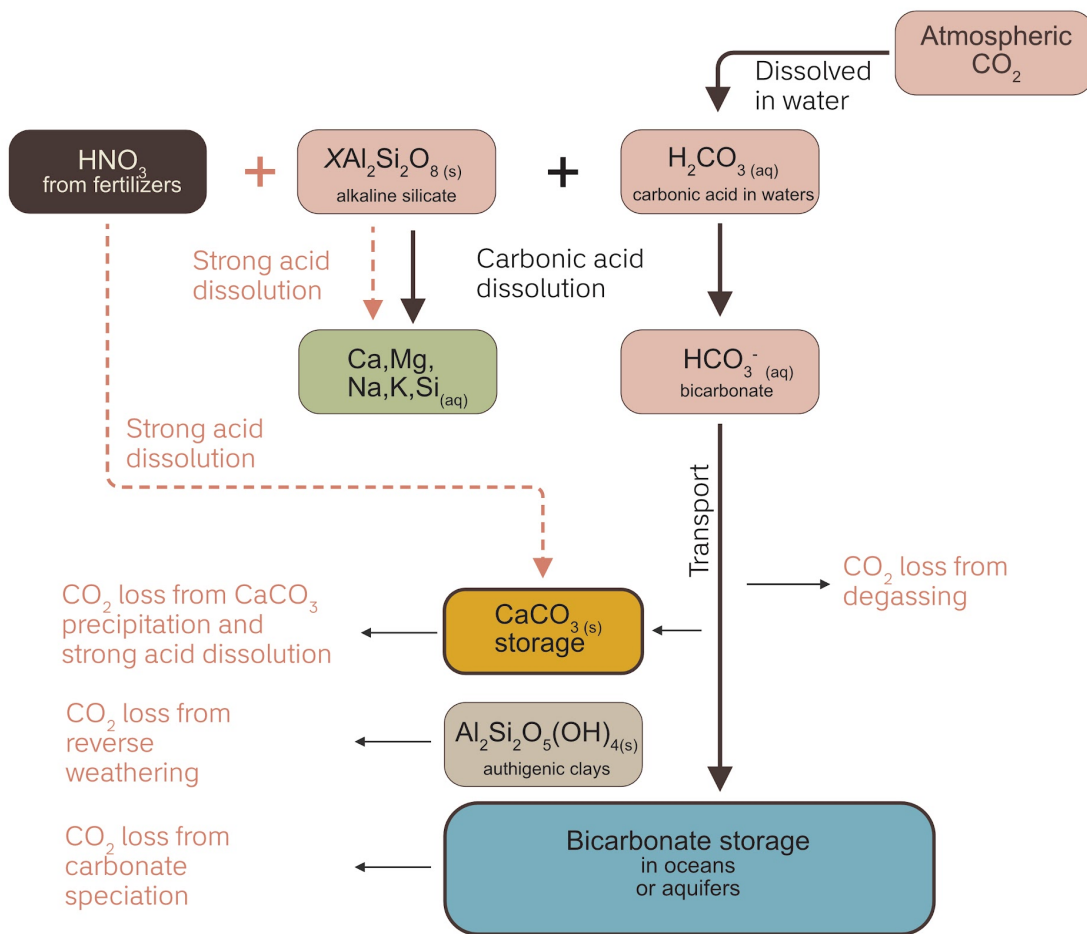


898

899 Fig 1. Illustration of conceptual stages for terrestrial EW CDR. The open system processes can be
900 broadly separated into three stages; i) capture, ii) transport and iii) storage. Note that there is spatial
901 and temporal overlap between the stages. The different stages give a modularity to CDR measurement
902 where we focus here on soil processes, with methods to estimate the primary capture stage of
903 bicarbonate formation.

904

905



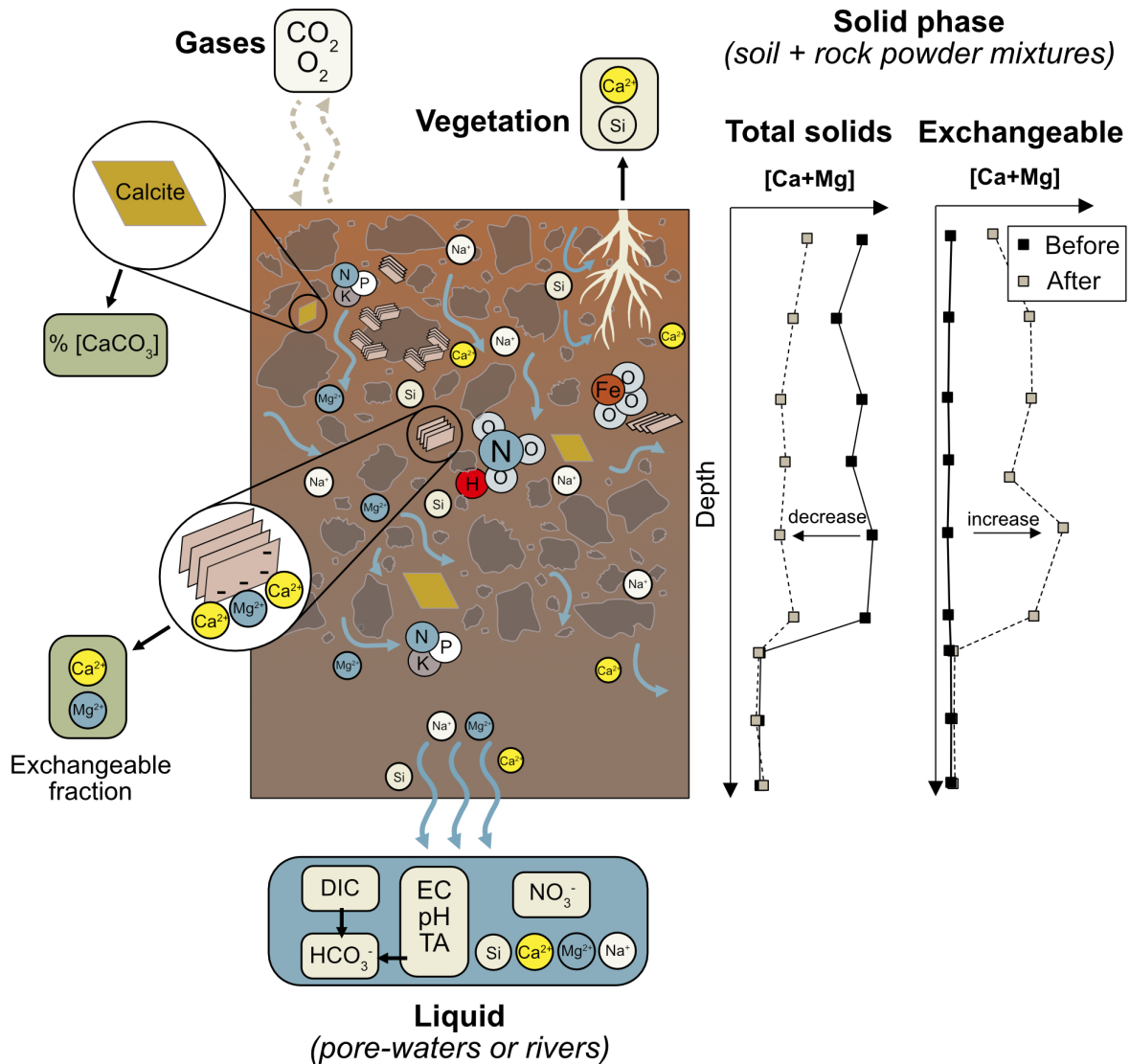
907

908 Fig. 2 Summary of the weathering process and potential complicating processes that result in
 909 downstream CO₂ loss. The primary aim of measurement techniques are to trace the loss or gain of
 910 weathering products in different phases; solid, liquid or gas. This can be relatively straightforward in
 911 cases where carbonic acid is the dominant weathering acid, but in cases where fertilizers produce
 912 nitric acid, weathering products may be released without concomitant CO₂ removal. Strong acids also
 913 drive carbonate dissolution that is a CO₂ source. CO₂ can also be lost during transport and at the final
 914 storage location, however a detailed review of these processes is beyond the scope of this paper.

915

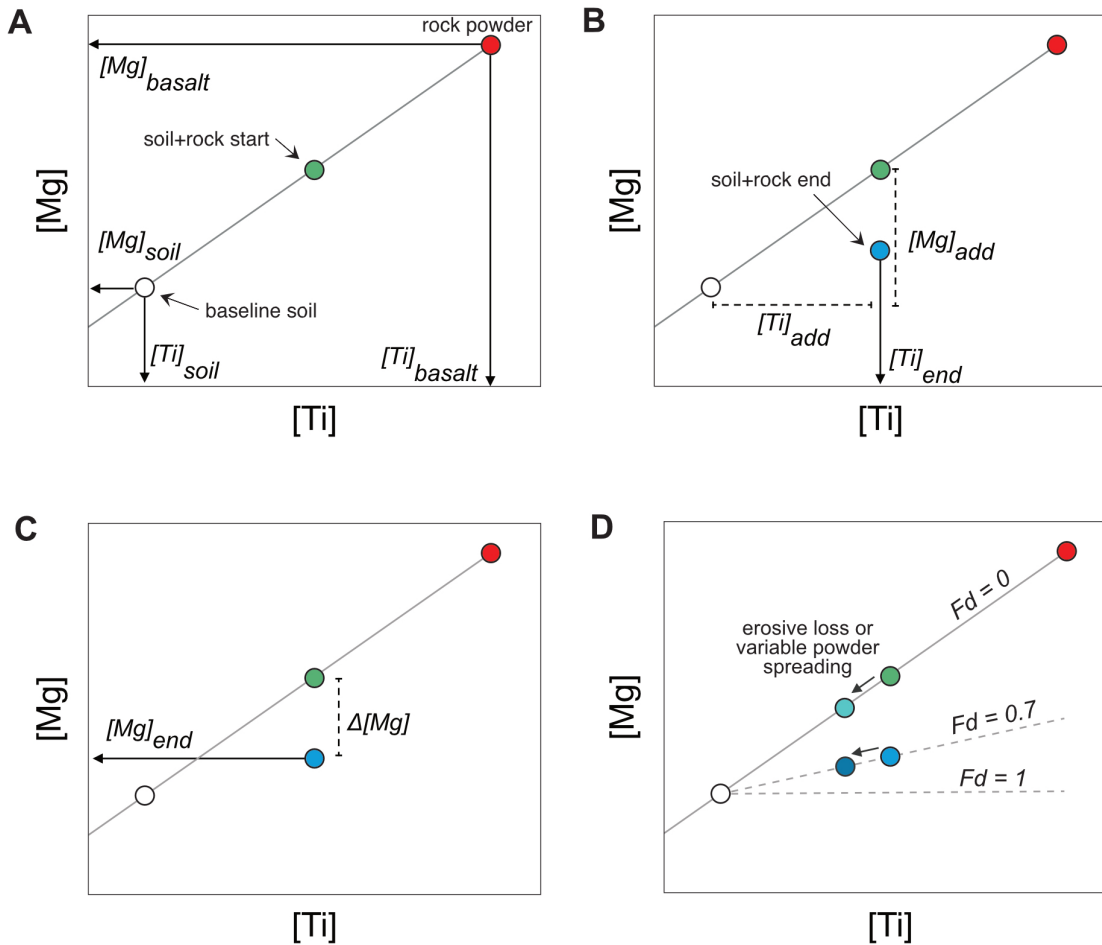
916

917



918

919 Fig. 3 Illustration of cation mass balance rooted in the concentration of an immobile trace element, Ti,
 920 modified from Reershemius, Kelland et al. (2024). Start and end values serve illustration purposes
 921 only and have not yet been measured. Here we show Mg as an example of a mobile cation, j. Panel A
 922 demonstrates the mixing line created by the baseline soil plus rock powder, where any combination of
 923 soil + rock powder would fall on this mixing line. B illustrates how a measure of immobile Ti at the
 924 end of weathering ($[Ti]_{end}$) can be used to calculate $[Mg]_{add}$. C illustrates the loss of $[Mg]$ during
 925 weathering, gained by the measurement of $[Mg]_{end}$, and is expressed as the change in $[Mg]$ ($\Delta[Mg]$). D
 926 demonstrates the cases where application amounts vary and weathering rates remain the same,
 927 meaning the fraction of $[Mg]$ lost relative to $Mg]_{add}$ (F_d), remains constant (dashed lines). Three
 928 examples are shown for no weathering ($F_d=0$), majority weathering ($F_d=0.7$) and complete
 929 weathering ($F_d=1$). Erosive loss of powder would be effectively the same as variable powder addition
 930 (D), illustrated by the sample moving toward $[Mg]_{soil}$, $[Ti]_{soil}$ with a slope of approximately constant
 931 F_d .

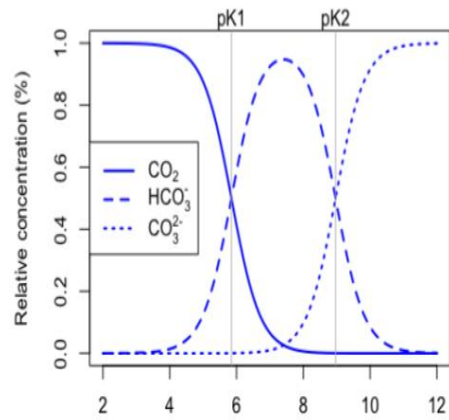


932

933 Fig. 4 Schematic view of approaches to monitoring weathering activity and idealized examples of
 934 total solid and exchangeable results. Different measurement pathways illustrate different components
 935 of the weathering mass balance, which must be comprehensively quantified to estimate weathering
 936 rates and calculate CDR. Data serve an illustrative purpose only and are not based on measurements.

937

938



939

940 Fig. 5. Bjerrum plot (created in RStudio with package seacarb and default values (Zeebe and
941 Wolf-Gladrow, 2001) showing the relative concentrations of carbonate species in solution. The typical
942 pH range for natural waters is indicated, where the dominant species of dissolved inorganic carbon is
943 HCO₃⁻.

944

946 **Tables**

947 Table 1 Comparison of the main methods to quantify EW. Methods are organized by the sample most commonly required to make the measurement type

Phase	Section	Basis	Advantages	Disadvantages
Solid samples	2.2.1 Maximum CDR potential of the feedstock	Uses the concentration of alkaline oxides in the feedstock to determine maximum amount of CO ₂ that could be stoichiometrically removed through dissolution	Useful for first considerations of feedstock choice	No temporal component Assumes complete weathering No consideration for acid type or CO ₂ losses
	2.2.2 Solid phase element mass balance	Examines cation concentrations in soil+rock powder mixtures to identify the loss of cations through dissolution. Cations measured in reference to immobile elements that remain in the soil.	Sampling soils aligns with agronomic practices Temporally integrated signals	Limited by measurement precision Limited by soil heterogeneity which can lead to large uncertainties No consideration for acid type or CO ₂ losses
	2.2.3 Accumulation of soil inorganic carbon	Measures the build up of soil inorganic carbon, which is one storage pool for capture carbon	Measure of captured and stored carbon via mineralization pathway Well established and standardized protocols	Does not include an estimate of bicarbonate capture or storage Limited to settings where carbonate precipitation occurs No consideration for acid type or CO ₂ losses
	2.3 Accumulation of	Quantifies cations that are temporarily stored in soil exchange sites	More clearly resolved differences compared to	Non-standardised chemical treatments, highly dependant on soil types

	weathering products in exchangeable phases		total solids	<p>No consideration for acid type or CO₂ losses</p> <p>Temporal fluctuations may bias/limit signals</p> <p>Assumes no leaching of cations occurs between sample intervals; cations lost to groundwater will not be detected as CDR</p>
Liquid samples	2.4.2 Base cations and dissolved silica	Quantifies the amount of rock powder dissolved by measuring the accumulation of weathering products in liquid samples (soil waters or rivers)	<p>Accurately identify flux of weathering products</p> <p>Spatially integrated if sampling rivers/drainage channels</p>	<p>Does not consider cations lost to the exchangeable fraction</p> <p>In some instances, limited scalability due to operational requirements</p> <p>Temporal fluctuations may bias/limit signals</p>
	2.4.3 Anions	Quantifies bicarbonate accumulation in liquid samples (soil waters or rivers)	<p>Direct measure of bicarbonate</p> <p>Identify non carbonic acids</p>	<p>In some instances, limited scalability due to operational requirements</p> <p>Temporal fluctuations may bias/limit signals</p>
	2.4.4 Total alkalinity, pH and DIC	Proxy measurement for bicarbonate accumulation in liquid samples (soil waters or rivers)	Closely linked to bicarbonate concentration	<p>Labour/skill intensive requiring careful sample handling</p> <p>Temporal fluctuations may bias/limit signals</p> <p>Can be influenced by respiration</p>

	2.4.5 Electrical Conductivity (EC)	Proxy measurement for total ion activity in liquid samples (soil waters or rivers)	Can be measured by sensors	Requires calibration of EC to alkalinity or cation concentrations
	2.5.2 Stable carbon and oxygen isotopes	Use isotope signatures to inform on the weathering mass balance (quantify sources and sinks)	Informs on additionality (i.e. C derived from non-air sources)	Some are expensive (radiocarbon) Complex interpretation
	2.5.3 Radiocarbon			
	2.5.4 Radiogenic strontium			
	2.5.5 Novel isotopes (Li, Mg, Si, stable Sr)	Use isotope signatures to inform on the weathering mass balance (quantify sources and sinks) and secondary processes	Detailed information on reaction processes, sources and sinks	Expensive Complex interpretation
Gas samples	2.6 Gaseous phases	Directly measurement of CO ₂ efflux in the soil system	Potential direct, in-situ measurement of CDR Can be combined with other GHG fluxes	Temporal fluctuations may bias/limit signals Dominated by organic carbon cycle and transient or short term carbon cycling

950 **References**

- 951 Alley, W. M. (1984). On the Treatment of Evapotranspiration, Soil Moisture Accounting, and Aquifer
 952 Recharge in Monthly Water Balance Models. *Water Resour. Res.* 20, 1137–1149. doi:
 953 10.1029/WR020i008p01137.
- 954 Alloway, B. J. ed. (2013). *Heavy Metals in Soils: Trace Metals and Metalloids in Soils and their*
 955 *Bioavailability*. Dordrecht: Springer Netherlands doi: 10.1007/978-94-007-4470-7.
- 956 Almaraz, M., Bingham, N. L., Holzer, I. O., Geoghegan, E. K., Goertzen, H., Sohng, J., et al. (2022).
 957 Methods for determining the CO₂ removal capacity of enhanced weathering in agronomic
 958 settings. *Front. Clim.* 4. Available at:
 959 <https://www.frontiersin.org/articles/10.3389/fclim.2022.970429> [Accessed October 16, 2023].
- 960 Amann, T., and Hartmann, J. (2022). Carbon Accounting for Enhanced Weathering. *Front. Clim.* 4.
 961 Available at: <https://www.frontiersin.org/articles/10.3389/fclim.2022.849948> [Accessed
 962 October 16, 2023].
- 963 Amann, T., Hartmann, J., Hellmann, R., Pedrosa, E. T., and Malik, A. (2022). Enhanced weathering
 964 potentials—the role of in situ CO₂ and grain size distribution. *Front. Clim.* 4. Available at:
 965 <https://www.frontiersin.org/articles/10.3389/fclim.2022.929268> [Accessed October 16, 2023].
- 966 Amann, T., Hartmann, J., Struyf, E., de Oliveira Garcia, W., Fischer, E. K., Janssens, I., et al. (2020).
 967 Enhanced Weathering and related element fluxes – a cropland mesocosm approach.
 968 *Biogeosciences* 17, 103–119. doi: 10.5194/bg-17-103-2020.
- 969 Andrews, M. G., Jacobson, A. D., Lehn, G. O., Horton, T. W., and Craw, D. (2016). Radiogenic and
 970 stable Sr isotope ratios (⁸⁷Sr/⁸⁶Sr, ⁸⁸Sr/⁸⁶Sr) as tracers of riverine cation sources and
 971 biogeochemical cycling in the Milford Sound region of Fiordland, New Zealand. *Geochim.*
 972 *Cosmochim. Acta* 173, 284–303. doi: 10.1016/j.gca.2015.10.005.
- 973 Andrews, M. G., and Taylor, L. L. (2019). Combating Climate Change Through Enhanced Weathering
 974 of Agricultural Soils. *Elements* 15, 253–258. doi: 10.2138/gselements.15.4.253.
- 975 Aubert, D., Stille, P., and Probst, A. (2001). REE fractionation during granite weathering and removal
 976 by waters and suspended loads: Sr and Nd isotopic evidence. *Geochim. Cosmochim. Acta* 65,
 977 387–406. doi: 10.1016/S0016-7037(00)00546-9.
- 978 Baek, S. H., Kanzaki, Y., Lora, J. M., Planavsky, N., Reinhard, C. T., and Zhang, S. (2023). Impact of
 979 Climate on the Global Capacity for Enhanced Rock Weathering on Croplands. *Earths Future*
 980 11, e2023EF003698. doi: 10.1029/2023EF003698.
- 981 Banwart, S. A., Berg, A., and Beerling, D. J. (2009). Process-based modeling of silicate mineral
 982 weathering responses to increasing atmospheric CO₂ and climate change. *Glob. Biogeochem.*
 983 *Cycles* 23. doi: 10.1029/2008GB003243.
- 984 Bayon, G., Bindeman, I. N., Trinquier, A., Retallack, G. J., and Bekker, A. (2022). Long-term
 985 evolution of terrestrial weathering and its link to Earth’s oxygenation. *Earth Planet. Sci. Lett.*
 986 584, 117490. doi: 10.1016/j.epsl.2022.117490.
- 987 Beerling, D. J., Kantzas, E. P., Lomas, M. R., Wade, P., Eufrazio, R. M., Renforth, P., et al. (2020).
 988 Potential for large-scale CO₂ removal via enhanced rock weathering with croplands. *Nature*
 989 583, 242–248. doi: 10.1038/s41586-020-2448-9.
- 990 Bergaya, F., Lagaly, G., and Vayer, M. (2006). “Chapter 12.10 Cation and Anion Exchange,” in
 991 *Developments in Clay Science Handbook of Clay Science.*, eds. F. Bergaya, B. K. G. Theng,
 992 and G. Lagaly (Elsevier), 979–1001. doi: 10.1016/S1572-4352(05)01036-6.
- 993 Berner, E. K., and Berner, R. A. (2012). “Global Environment: Water, Air, and Geochemical Cycles -
 994 Second Edition,” in *Global Environment* (Princeton University Press). doi:
 995 10.1515/9781400842766.
- 996 Berner, R. A., Lasaga, A. C., and Garrels, R. M. (1983). Carbonate-silicate geochemical cycle and its
 997 effect on atmospheric carbon dioxide over the past 100 million years. *Am J Sci United States*
 998 283.
- 999 Bhatia, M. P., Kujawinski, E. B., Das, S. B., Breier, C. F., Henderson, P. B., and Charette, M. A.

- 1000 (2013). Greenland meltwater as a significant and potentially bioavailable source of iron to the
1001 ocean. *Nat. Geosci.* 6, 274–278. doi: 10.1038/ngeo1746.
- 1002 Blum, J. D., and Erel, Y. (2003). “5.12 - Radiogenic Isotopes in Weathering and Hydrology,” in
1003 *Treatise on Geochemistry*, eds. H. D. Holland and K. K. Turekian (Oxford: Pergamon),
1004 365–392. doi: 10.1016/B0-08-043751-6/05082-9.
- 1005 Brady, N. C., and Weil, R. R. (2008). *The Nature and Properties of Soils*. Pearson Prentice Hall.
- 1006 Brander, M., Ascui, F., Scott, V., and Tett, S. (2021). Carbon accounting for negative emissions
1007 technologies. *Clim. Policy* 21, 699–717. doi: 10.1080/14693062.2021.1878009.
- 1008 Brantley, S. L., Shaughnessy, A., Lebedeva, M. I., and Balashov, V. N. (2023). How
1009 temperature-dependent silicate weathering acts as Earth’s geological thermostat. *Science* 379,
1010 382–389. doi: 10.1126/science.add2922.
- 1011 Brimhall, G. H., and Dietrich, W. E. (1987). Constitutive mass balance relations between chemical
1012 composition, volume, density, porosity, and strain in metasomatic hydrochemical systems:
1013 Results on weathering and pedogenesis. *Geochim. Cosmochim. Acta* 51, 567–587. doi:
1014 10.1016/0016-7037(87)90070-6.
- 1015 Britto, D. T., and Kronzucker, H. J. (2008). Cellular mechanisms of potassium transport in plants.
1016 *Physiol. Plant.* 133, 637–650. doi: 10.1111/j.1399-3054.2008.01067.x.
- 1017 Brown, I. C. (1943). A rapid method of determining exchangeable hydrogen and total exchangeable
1018 bases of soils. *Soil Sci.* 56, 353–358.
- 1019 Brune, A., Urbach, W., and Dietz, K.-J. (1995). Differential toxicity of heavy metals is partly related
1020 to a loss of preferential extraplasmic compartmentation: a comparison of Cd-, Mo-, Ni- and
1021 Zn-stress. *New Phytol.* 129, 403–409.
- 1022 Calabrese, S., Parolari, A. J., and Porporato, A. (2017). Hydrologic Transport of Dissolved Inorganic
1023 Carbon and Its Control on Chemical Weathering. *J. Geophys. Res. Earth Surf.* 122,
1024 2016–2032. doi: 10.1002/2017JF004346.
- 1025 Calabrese, S., Wild, B., Bertagni, M. B., Bourg, I. C., White, C., Aburto, F., et al. (2022). Nano-to
1026 global-scale uncertainties in terrestrial enhanced weathering. *Environ. Sci. Technol.* 56,
1027 15261–15272.
- 1028 Campbell, J., Bastianini, L., Buckman, J., Bullock, L., Foteinis, S., Furey, V., et al. (2023).
1029 Measurements in Geochemical Carbon Dioxide Removal. Heriot-Watt University doi:
1030 10.17861/2GE7-RE08.
- 1031 Campbell, J. S., Foteinis, S., Furey, V., Hawrot, O., Pike, D., Aeschlimann, S., et al. (2022).
1032 Geochemical Negative Emissions Technologies: Part I. Review. *Front. Clim.* 4. Available at:
1033 <https://www.frontiersin.org/articles/10.3389/fclim.2022.879133> [Accessed October 16, 2023].
- 1034 Carbon Standards International (CSI) (2022). Global Rock C-Sink. Available at:
1035 https://www.european-biochar.org/media/doc/139/rock-c-guidelines_0_9.pdf [Accessed
1036 October 26, 2023].
- 1037 Cerling, T. E. (1984). The stable isotopic composition of modern soil carbonate and its relationship to
1038 climate. *Earth Planet. Sci. Lett.* 71, 229–240. doi: 10.1016/0012-821X(84)90089-X.
- 1039 Chiaravalloti, I., Theunissen, N., Zhang, S., Wang, J., Sun, F., Ahmed, A. A., et al. (2023). Mitigation
1040 of soil nitrous oxide emissions during maize production with basalt amendments. *Front. Clim.*
1041 5. Available at: <https://www.frontiersin.org/articles/10.3389/fclim.2023.1203043> [Accessed
1042 November 22, 2023].
- 1043 Cipolla, G., Calabrese, S., Noto, L. V., and Porporato, A. (2021). The role of hydrology on enhanced
1044 weathering for carbon sequestration II. From hydroclimatic scenarios to carbon-sequestration
1045 efficiencies. *Adv. Water Resour.* 154, 103949. doi: 10.1016/j.advwatres.2021.103949.
- 1046 Cipolla, G., Calabrese, S., Porporato, A., and Noto, L. V. (2022). Effects of precipitation seasonality,
1047 irrigation, vegetation cycle and soil type on enhanced weathering – modeling of cropland case
1048 studies across four sites. *Biogeosciences* 19, 3877–3896. doi: 10.5194/bg-19-3877-2022.
- 1049 Dietzen, C., Harrison, R., and Michelsen-Correa, S. (2018). Effectiveness of enhanced mineral
1050 weathering as a carbon sequestration tool and alternative to agricultural lime: An incubation
1051 experiment. *Int. J. Greenh. Gas Control* 74, 251–258. doi: 10.1016/j.ijggc.2018.05.007.
- 1052 Dietzen, C., and Rosing, M. T. (2023). Quantification of CO₂ uptake by enhanced weathering of
1053 silicate minerals applied to acidic soils. *Int. J. Greenh. Gas Control* 125, 103872. doi:
1054 10.1016/j.ijggc.2023.103872.

- 1055 Dudhaiya, A., Haque, F., Fantucci, H., and Santos, R. M. (2019). Characterization of physically
1056 fractionated wollastonite-amended agricultural soils. *Minerals* 9, 635.
- 1057 Dupla, X., Möller, B., Baveye, P. C., and Grand, S. (2023). Potential accumulation of toxic trace
1058 elements in soils during enhanced rock weathering. *Eur. J. Soil Sci.* 74, e13343.
- 1059 Eufrazio, R. M., Kantzas, E. P., Edwards, N. R., Holden, P. B., Pollitt, H., Mercure, J.-F., et al. (2022).
1060 Environmental and health impacts of atmospheric CO₂ removal by enhanced rock weathering
1061 depend on nations' energy mix. *Commun. Earth Environ.* 3, 106.
- 1062 Faure, G., and Mensing, T. M. (2005). *Principles and Applications*. John Wiley & Sons, Inc.
- 1063 Fritz, S. J. (1994). A Survey of Charge-Balance Errors on Published Analyses of Potable Ground and
1064 Surface Waters. *Groundwater* 32, 539–546. doi: 10.1111/j.1745-6584.1994.tb00888.x.
- 1065 Fuhr, M., Geilert, S., Schmidt, M., Liebetrau, V., Vogt, C., Ledwig, B., et al. (2022). Kinetics of
1066 Olivine Weathering in Seawater: An Experimental Study. *Front. Clim.* 4. Available at:
1067 <https://www.frontiersin.org/articles/10.3389/fclim.2022.831587> [Accessed October 19, 2023].
- 1068 Fuss, S., Lamb, W. F., Callaghan, M. W., Hilaire, J., Creutzig, F., Amann, T., et al. (2018). Negative
1069 emissions—Part 2: Costs, potentials and side effects. *Environ. Res. Lett.* 13, 063002. doi:
1070 10.1088/1748-9326/aabf9f.
- 1071 Gaillardet, J., Dupré, B., and Allègre, C. J. (1999a). Geochemistry of large river suspended sediments:
1072 silicate weathering or recycling tracer? *Geochim. Cosmochim. Acta* 63, 4037–4051. doi:
1073 10.1016/S0016-7037(99)00307-5.
- 1074 Gaillardet, J., Dupré, B., Louvat, P., and Allègre, C. J. (1999b). Global silicate weathering and CO₂
1075 consumption rates deduced from the chemistry of large rivers. *Chem. Geol.* 159, 3–30. doi:
1076 10.1016/S0009-2541(99)00031-5.
- 1077 Galy, A., and France-Lanord, C. (1999). Weathering processes in the Ganges–Brahmaputra basin and
1078 the riverine alkalinity budget. *Chem. Geol.* 159, 31–60. doi:
1079 10.1016/S0009-2541(99)00033-9.
- 1080 Goll, D. S., Ciais, P., Amann, T., Buermann, W., Chang, J., Eker, S., et al. (2021). Potential CO₂
1081 removal from enhanced weathering by ecosystem responses to powdered rock. *Nat. Geosci.*
1082 14, 545–549. doi: 10.1038/s41561-021-00798-x.
- 1083 Gran, G. (1952). Determination of the equivalence point in potentiometric titrations. Part II. *Analyst*
1084 77, 661–671. doi: 10.1039/AN9527700661.
- 1085 Groenenberg, J. E., Römkens, P. F., Zomer, A. V., Rodrigues, S. M., and Comans, R. N. (2017).
1086 Evaluation of the single dilute (0.43 M) nitric acid extraction to determine geochemically
1087 reactive elements in soil. *Environ. Sci. Technol.* 51, 2246–2253.
- 1088 Hamilton, S. K., Kurzman, A. L., Arango, C., Jin, L., and Robertson, G. P. (2007). Evidence for
1089 carbon sequestration by agricultural liming. *Glob. Biogeochem. Cycles* 21. doi:
1090 10.1029/2006GB002738.
- 1091 Haque, F., Khalidy, R., Chiang, Y. W., and Santos, R. M. (2023). Constraining the Capacity of Global
1092 Croplands to CO₂ Drawdown via Mineral Weathering. *ACS Earth Space Chem.* 7,
1093 1294–1305. doi: 10.1021/acsearthspacechem.2c00374.
- 1094 Haque, F., Santos, R. M., and Chiang, Y. W. (2020). CO₂ sequestration by wollastonite-amended
1095 agricultural soils – An Ontario field study. *Int. J. Greenh. Gas Control* 97, 103017. doi:
1096 10.1016/j.ijggc.2020.103017.
- 1097 Haque, F., Santos, R. M., Dutta, A., Thimmanagari, M., and Chiang, Y. W. (2019). Co-Benefits of
1098 Wollastonite Weathering in Agriculture: CO₂ Sequestration and Promoted Plant Growth. *ACS*
1099 *Omega* 4, 1425–1433. doi: 10.1021/acsomega.8b02477.
- 1100 Harrington, K. J., Hilton, R. G., and Henderson, G. M. (2023). Implications of the Riverine Response
1101 to Enhanced Weathering for CO₂ removal in the UK. *Appl. Geochem.* 152, 105643. doi:
1102 10.1016/j.apgeochem.2023.105643.
- 1103 Harris, N., Bickle, M., Chapman, H., Fairchild, I., and Judith Bunbury (1998). The significance of
1104 Himalayan rivers for silicate weathering rates: evidence from the Bhothe Kosi tributary. *Chem.*
1105 *Geol.* 144, 205–220. doi: 10.1016/S0009-2541(97)00132-0.
- 1106 Hartmann, J., Lauerwald, R., and Moosdorf, N. (2014). A Brief Overview of the GLObal RIVER
1107 Chemistry Database, GLORICH. *Procedia Earth Planet. Sci.* 10, 23–27. doi:
1108 10.1016/j.proeps.2014.08.005.
- 1109 Hartmann, J., West, A. J., Renforth, P., Köhler, P., De La Rocha, C. L., Wolf-Gladrow, D. A., et al.

- 1110 (2013). Enhanced chemical weathering as a geoengineering strategy to reduce atmospheric
 1111 carbon dioxide, supply nutrients, and mitigate ocean acidification. *Rev. Geophys.* 51,
 1112 113–149. doi: 10.1002/rog.20004.
- 1113 Hilton, R. G., and West, A. J. (2020). Mountains, erosion and the carbon cycle. *Nat. Rev. Earth*
 1114 *Environ.* 1, 284–299. doi: 10.1038/s43017-020-0058-6.
- 1115 Holzer, I. O., Nocco, M. A., and Houlton, B. Z. (2023a). Direct evidence for atmospheric carbon
 1116 dioxide removal via enhanced weathering in cropland soil. *Environ. Res. Commun.* 5, 101004.
 1117 doi: 10.1088/2515-7620/acfd89.
- 1118 Holzer, I., Sokol, N., Slessarev, E., Martin, K., and Chay, F. (2023b). Quantifying enhanced
 1119 weathering – CarbonPlan. Available at:
 1120 <https://carbonplan.org/research/ew-quantification-explainer> [Accessed October 16, 2023].
- 1121 Horan, K., Hilton, R. G., Dellinger, M., Tipper, E., Galy, V., Calmels, D., et al. (2019). Carbon dioxide
 1122 emissions by rock organic carbon oxidation and the net geochemical carbon budget of the
 1123 Mackenzie River Basin. *Am. J. Sci.* 319, 473–499. doi: 10.2475/06.2019.02.
- 1124 IPCC (2022). *Climate Change 2022: Impacts, Adaptation and Vulnerability. Contribution of Working*
 1125 *Group III to the Sixth Assessment Report of the Intergovernmental Panel on Climate Change.*
 1126 , eds. P. R. Shukla, J. Skea, R. Slade, A. Al Khourdajie, R. van Diemen, D. McCollum, et al.
 1127 doi: 10.1017/9781009157926.
- 1128 Isson, T. T., and Planavsky, N. J. (2018). Reverse weathering as a long-term stabilizer of marine pH
 1129 and planetary climate. *Nature* 560, 471–475. doi: 10.1038/s41586-018-0408-4.
- 1130 Jacobson, A. D., Blum, J. D., and Walter, L. M. (2002). Reconciling the elemental and Sr isotope
 1131 composition of Himalayan weathering fluxes: insights from the carbonate geochemistry of
 1132 stream waters. *Geochim. Cosmochim. Acta* 66, 3417–3429. doi:
 1133 10.1016/S0016-7037(02)00951-1.
- 1134 Kantola, I. B., Blanc-Betes, E., Masters, M. D., Chang, E., Marklein, A., Moore, C. E., et al. (2023).
 1135 Improved net carbon budgets in the US Midwest through direct measured impacts of
 1136 enhanced weathering. *Glob. Change Biol.* n/a. doi: 10.1111/gcb.16903.
- 1137 Kantzas, E. P., Val Martin, M., Lomas, M. R., Eufrazio, R. M., Renforth, P., Lewis, A. L., et al.
 1138 (2022). Substantial carbon drawdown potential from enhanced rock weathering in the United
 1139 Kingdom. *Nat. Geosci.* 15, 382–389. doi: 10.1038/s41561-022-00925-2.
- 1140 Kanzaki, Y., Planavsky, N. J., and Reinhard, C. T. (2023). New estimates of the storage permanence
 1141 and ocean co-benefits of enhanced rock weathering. *PNAS Nexus* 2, pgad059. doi:
 1142 10.1093/pnasnexus/pgad059.
- 1143 Kanzaki, Y., Zhang, S., Planavsky, N. J., and Reinhard, C. T. (2022). Soil Cycles of Elements
 1144 simulator for Predicting TERrestrial regulation of greenhouse gases: SCEPTER v0.9. *Geosci.*
 1145 *Model Dev.* 15, 4959–4990. doi: 10.5194/gmd-15-4959-2022.
- 1146 Kelland, M. E., Wade, P. W., Lewis, A. L., Taylor, L. L., Sarkar, B., Andrews, M. G., et al. (2020).
 1147 Increased yield and CO₂ sequestration potential with the C₄ cereal *Sorghum bicolor*
 1148 cultivated in basaltic rock dust-amended agricultural soil. *Glob. Change Biol.* 26, 3658–3676.
 1149 doi: 10.1111/gcb.15089.
- 1150 Kemp, S. J., Lewis, A. L., and Rushton, J. C. (2022). Detection and quantification of low levels of
 1151 carbonate mineral species using thermogravimetric-mass spectrometry to validate CO₂
 1152 drawdown via enhanced rock weathering. *Appl. Geochem.* 146, 105465. doi:
 1153 10.1016/j.apgeochem.2022.105465.
- 1154 Kerr, D. E., Brown, P. J., Grey, A., and Kelleher, B. P. (2021). The influence of organic alkalinity on
 1155 the carbonate system in coastal waters. *Mar. Chem.* 237, 104050. doi:
 1156 10.1016/j.marchem.2021.104050.
- 1157 Khalidy, R., Haque, F., Chiang, Y. W., and Santos, R. M. (2021). Monitoring Pedogenic Inorganic
 1158 Carbon Accumulation Due to Weathering of Amended Silicate Minerals in Agricultural Soils.
 1159 *J Vis Exp.* doi: 10.3791/61996.
- 1160 Klitzke, J., Hausfather, Z., and Ransohoff, N. (2022). Quantifying delivered carbon removal as a
 1161 buyer of early technologies. Available at:
 1162 <https://frontierclimate.com/writing/quantifying-delivered-cdr> [Accessed November 21, 2023].
- 1163 Knapp, W. J., Stevenson, E. I., Renforth, P., Ascough, P. L., Knight, A. C. G., Bridgestock, L., et al.
 1164 (2023). Quantifying CO₂ Removal at Enhanced Weathering Sites: a Multiproxy Approach.

1165 *Environ. Sci. Technol.* 57, 9854–9864. doi: 10.1021/acs.est.3c03757.

1166 Knapp, W. J., and Tipper, E. T. (2022). The efficacy of enhancing carbonate weathering for carbon
1167 dioxide sequestration. *Front. Clim.* 4. Available at:
1168 <https://www.frontiersin.org/articles/10.3389/fclim.2022.928215> [Accessed October 16, 2023].

1169 Köhler, P., Hartmann, J., and Wolf-Gladrow, D. A. (2010). Geoengineering potential of artificially
1170 enhanced silicate weathering of olivine. *Proc. Natl. Acad. Sci.* 107, 20228–20233. doi:
1171 10.1073/pnas.1000545107.

1172 Larkin, C. S., Andrews, M. G., Pearce, C. R., Yeong, K. L., Beerling, D. J., Bellamy, J., et al. (2022).
1173 Quantification of CO₂ removal in a large-scale enhanced weathering field trial on an oil palm
1174 plantation in Sabah, Malaysia. *Front. Clim.* 4. Available at:
1175 <https://www.frontiersin.org/articles/10.3389/fclim.2022.959229> [Accessed October 16, 2023].

1176 Larkin, C. S., Piotrowski, A. M., Hindshaw, R. S., Bayon, G., Hilton, R. G., Baronas, J. J., et al.
1177 (2021). Constraints on the source of reactive phases in sediment from a major Arctic river
1178 using neodymium isotopes. *Earth Planet. Sci. Lett.* 565, 116933. doi:
1179 10.1016/j.epsl.2021.116933.

1180 Lefebvre, D., Goglio, P., Williams, A., Manning, D. A., de Azevedo, A. C., Bergmann, M., et al.
1181 (2019). Assessing the potential of soil carbonation and enhanced weathering through Life
1182 Cycle Assessment: A case study for Sao Paulo State, Brazil. *J. Clean. Prod.* 233, 468–481.

1183 Lerman, A., and Wu, L. (2006). CO₂ and sulfuric acid controls of weathering and river water
1184 composition. *J. Geochem. Explor.* 88, 427–430. doi: 10.1016/j.gexplo.2005.08.100.

1185 Lewis, A. L., Sarkar, B., Wade, P., Kemp, S. J., Hodson, M. E., Taylor, L. L., et al. (2021). Effects of
1186 mineralogy, chemistry and physical properties of basalts on carbon capture potential and
1187 plant-nutrient element release via enhanced weathering. *Appl. Geochem.* 132, 105023. doi:
1188 10.1016/j.apgeochem.2021.105023.

1189 Maesano, C. N., Campbell, J. S., Foteinis, S., Furey, V., Hawrot, O., Pike, D., et al. (2022).
1190 Geochemical Negative Emissions Technologies: Part II. Roadmap. *Front. Clim.* 4. Available
1191 at: <https://www.frontiersin.org/articles/10.3389/fclim.2022.945332> [Accessed October 16,
1192 2023].

1193 Manning, D. A. C., Renforth, P., Lopez-Capel, E., Robertson, S., and Ghazireh, N. (2013). Carbonate
1194 precipitation in artificial soils produced from basaltic quarry fines and composts: An
1195 opportunity for passive carbon sequestration. *Int. J. Greenh. Gas Control* 17, 309–317. doi:
1196 10.1016/j.ijggc.2013.05.012.

1197 Manning, D. A. C., and Theodoro, S. H. (2020). Enabling food security through use of local rocks and
1198 minerals. *Extr. Ind. Soc.* 7, 480–487. doi: 10.1016/j.exis.2018.11.002.

1199 McCabe, G. J., and Markstrom, S. L. (2007). A monthly water-balance model driven by a graphical
1200 user interface. U.S. Geological Survey doi: 10.3133/ofr20071088.

1201 Meybeck, M. (1982). Carbon, nitrogen, and phosphorus transport by world rivers. *Am J Sci U. S.*
1202 282:4. doi: 10.2475/ajs.282.4.401.

1203 Moatar, F., and Meybeck, M. (2005). Compared performances of different algorithms for estimating
1204 annual nutrient loads discharged by the eutrophic River Loire. *Hydrol. Process.* 19, 429–444.
1205 doi: 10.1002/hyp.5541.

1206 Moon, S., Chamberlain, C. P., and Hilley, G. E. (2014). New estimates of silicate weathering rates and
1207 their uncertainties in global rivers. *Geochim. Cosmochim. Acta* 134, 257–274. doi:
1208 10.1016/j.gca.2014.02.033.

1209 Mu, L., Palter, J. B., and Wang, H. (2023). Considerations for hypothetical carbon dioxide removal
1210 via alkalinity addition in the Amazon River watershed. *Biogeosciences* 20, 1963–1977. doi:
1211 10.5194/bg-20-1963-2023.

1212 Négrel, P., Allègre, C. J., Dupré, B., and Lewin, E. (1993). Erosion sources determined by inversion
1213 of major and trace element ratios and strontium isotopic ratios in river water: The Congo
1214 Basin case. *Earth Planet. Sci. Lett.* 120, 59–76. doi: 10.1016/0012-821X(93)90023-3.

1215 Nunes, J. M. G., Kautzmann, R. M., and Oliveira, C. (2014). Evaluation of the natural fertilizing
1216 potential of basalt dust wastes from the mining district of Nova Prata (Brazil). *J. Clean. Prod.*
1217 84, 649–656. doi: <https://doi.org/10.1016/j.jclepro.2014.04.032>.

1218 Oelkers, E. H., Pogge von Strandmann, P. A. E., and Mavromatis, V. (2019). The rapid resetting of the
1219 Ca isotopic signatures of calcite at ambient temperature during its congruent dissolution,

1220 precipitation, and at equilibrium. *Chem. Geol.* 512, 1–10. doi:
1221 10.1016/j.chemgeo.2019.02.035.

1222 Paessler, D., Steffens, R., Hammes, J., and Smet, I. (2023). Monitoring CO₂ Concentrations in Soil
1223 Gas - A Novel MRV Approach for Cropland-Based Enhanced Rock Weathering (ERW)
1224 (compressed).pdf. *Carbon Draw. Initiat.* Available at:
1225 [https://www.carbon-drawdown.de/blog/2023-5-17-monitoring-co2-concentrations-in-soil-gas-](https://www.carbon-drawdown.de/blog/2023-5-17-monitoring-co2-concentrations-in-soil-gas-a-novel-mrv-approach-for-cropland-based-erw)
1226 [a-novel-mrv-approach-for-cropland-based-erw](https://www.carbon-drawdown.de/blog/2023-5-17-monitoring-co2-concentrations-in-soil-gas-a-novel-mrv-approach-for-cropland-based-erw) [Accessed November 24, 2023].

1227 Parkhurst, D. L. (1995). *User's guide to PHREEQC: A computer program for speciation,*
1228 *reaction-path, advective-transport, and inverse geochemical calculations.* US Department of
1229 the Interior, US Geological Survey.

1230 Penniston-Dorland, S., Liu, X.-M., and Rudnick, R. L. (2017). Lithium Isotope Geochemistry. *Rev.*
1231 *Mineral. Geochem.* 82, 165–217. doi: 10.2138/rmg.2017.82.6.

1232 Perrin, A.-S., Probst, A., and Probst, J.-L. (2008). Impact of nitrogenous fertilizers on carbonate
1233 dissolution in small agricultural catchments: Implications for weathering CO₂ uptake at
1234 regional and global scales. *Geochim. Cosmochim. Acta* 72, 3105–3123. doi:
1235 10.1016/j.gca.2008.04.011.

1236 Pogge von Strandmann, P. A. E., Fraser, W. T., Hammond, S. J., Tarbuck, G., Wood, I. G., Oelkers, E.
1237 H., et al. (2019). Experimental determination of Li isotope behaviour during basalt
1238 weathering. *Chem. Geol.* 517, 34–43. doi: 10.1016/j.chemgeo.2019.04.020.

1239 Pogge von Strandmann, P. A. E., Renforth, P., West, A. J., Murphy, M. J., Luu, T.-H., and Henderson,
1240 G. M. (2021). The lithium and magnesium isotope signature of olivine dissolution in soil
1241 experiments. *Chem. Geol.* 560, 120008. doi: 10.1016/j.chemgeo.2020.120008.

1242 Puro.earth (2022). Enhanced Rock Weathering Methodology. Available at:
1243 [https://7518557.fs1.hubspotusercontent-na1.net/hubfs/7518557/Supplier%20Documents/ER](https://7518557.fs1.hubspotusercontent-na1.net/hubfs/7518557/Supplier%20Documents/ERW%20methodology.pdf)
1244 [W%20methodology.pdf](https://7518557.fs1.hubspotusercontent-na1.net/hubfs/7518557/Supplier%20Documents/ERW%20methodology.pdf) [Accessed October 26, 2023].

1245 Rausis, K., Stubbs, A. R., Power, I. M., and Paulo, C. (2022). Rates of atmospheric CO₂ capture using
1246 magnesium oxide powder. *Int. J. Greenh. Gas Control* 119, 103701. doi:
1247 10.1016/j.ijggc.2022.103701.

1248 Reershemius, T., Kelland, M. E., Jordan, J. S., Davis, I. R., D'Ascanio, R., Kalderon-Asael, B., et al.
1249 (2023). Initial Validation of a Soil-Based Mass-Balance Approach for Empirical Monitoring
1250 of Enhanced Rock Weathering Rates. *Environ. Sci. Technol.* doi: 10.1021/acs.est.3c03609.

1251 Reershemius, T., and Suhrhoff, T. J. (2023). On error, uncertainty, and assumptions in calculating
1252 carbon dioxide removal rates by enhanced rock weathering in Kantola et al., 2023. *Glob.*
1253 *Change Biol.* n/a, e17025. doi: 10.1111/gcb.17025.

1254 Reiman, J. H., and Xu, Y. J. (2019). Dissolved carbon export and CO₂ outgassing from the lower
1255 Mississippi River – Implications of future river carbon fluxes. *J. Hydrol.* 578, 124093. doi:
1256 10.1016/j.jhydrol.2019.124093.

1257 Relph, K. E., Stevenson, E. I., Turchyn, A. V., Antler, G., Bickle, M. J., Baronas, J. J., et al. (2021).
1258 Partitioning riverine sulfate sources using oxygen and sulfur isotopes: Implications for carbon
1259 budgets of large rivers. *Earth Planet. Sci. Lett.* 567, 116957. doi: 10.1016/j.epsl.2021.116957.

1260 Renforth, P. (2012). The potential of enhanced weathering in the UK. *Int. J. Greenh. Gas Control* 10,
1261 229–243.

1262 Renforth, P. (2019). The negative emission potential of alkaline materials. *Nat. Commun.* 10, 1401.
1263 doi: 10.1038/s41467-019-09475-5.

1264 Renforth, P., and Campbell, J. S. (2021). The role of soils in the regulation of ocean acidification.
1265 *Philos. Trans. R. Soc. B Biol. Sci.* 376, 20200174. doi: 10.1098/rstb.2020.0174.

1266 Renforth, P., and Henderson, G. (2017). Assessing ocean alkalinity for carbon sequestration. *Rev.*
1267 *Geophys.* 55, 636–674.

1268 Renforth, P., Manning, D. A. C., and Lopez-Capel, E. (2009). Carbonate precipitation in artificial soils
1269 as a sink for atmospheric carbon dioxide. *Appl. Geochem.* 24, 1757–1764. doi:
1270 10.1016/j.apgeochem.2009.05.005.

1271 Renforth, P., Pogge von Strandmann, P. A. E., and Henderson, G. M. (2015). The dissolution of
1272 olivine added to soil: Implications for enhanced weathering. *Appl. Geochem.* 61, 109–118.
1273 doi: 10.1016/j.apgeochem.2015.05.016.

1274 Santos, R. M., Araujo, F., Jariwala, H., Khalidy, R., Haque, F., and Chiang, Y. W. (2023). Pathways,

1275 roundabouts, roadblocks, and shortcuts to safe and sustainable deployment of enhanced rock
1276 weathering in agriculture. *Front. Earth Sci.* 11. Available at:
1277 <https://www.frontiersin.org/articles/10.3389/feart.2023.1215930> [Accessed October 16,
1278 2023].

1279 Schuiling, R. D., and Krijgsman, P. (2006). Enhanced Weathering: An Effective and Cheap Tool to
1280 Sequester Co₂. *Clim. Change* 74, 349–354. doi: 10.1007/s10584-005-3485-y.

1281 Schuiling, R. D., Wilson, S., and Power, Ian M. (2011). Enhanced silicate weathering is not limited
1282 by silicic acid saturation. *Proc. Natl. Acad. Sci.* 108, E41–E41. doi:
1283 10.1073/pnas.1019024108.

1284 Schulte, P., van Geldern, R., Freitag, H., Karim, A., Négrel, P., Petelet-Giraud, E., et al. (2011).
1285 Applications of stable water and carbon isotopes in watershed research: Weathering, carbon
1286 cycling, and water balances. *Earth-Sci. Rev.* 109, 20–31. doi: 10.1016/j.earscirev.2011.07.003.

1287 Seifritz, W. (1990). CO₂ disposal by means of silicates. *Nature* 345, 486–486. doi:
1288 10.1038/345486b0.

1289 Shao, S., Driscoll, C. T., Johnson, C. E., Fahey, T. J., Battles, J. J., and Blum, J. D. (2015). Long-term
1290 responses in soil solution and stream-water chemistry at Hubbard Brook after experimental
1291 addition of wollastonite. *Environ. Chem.* 13, 528–540.

1292 Slessarev, E. W., Chadwick, O. A., Sokol, N. W., Nuccio, E. E., and Pett-Ridge, J. (2022). Rock
1293 weathering controls the potential for soil carbon storage at a continental scale.
1294 *Biogeochemistry* 157, 1–13. doi: 10.1007/s10533-021-00859-8.

1295 Smith, S. M., Geden, O., Nemet, G. F., Gidden, M. J., Lamb, W. F., Powis, C., et al. (2023). The State
1296 of Carbon Dioxide Removal - 1st Edition. The State of Carbon Dioxide Removal doi:
1297 10.17605/OSF.IO/W3B4Z.

1298 Stubbs, A. R., Paulo, C., Power, I. M., Wang, B., Zeyen, N., and Wilson, S. (2022). Direct
1299 measurement of CO₂ drawdown in mine wastes and rock powders: Implications for enhanced
1300 rock weathering. *Int. J. Greenh. Gas Control* 113, 103554. doi: 10.1016/j.ijggc.2021.103554.

1301 Stubbs, A. R., Power, I. M., Paulo, C., Wang, B., Zeyen, N., Wilson, S., et al. (2023). Impact of
1302 wet-dry cycles on enhanced rock weathering of brucite, wollastonite, serpentinite and
1303 kimberlite: Implications for carbon verification. *Chem. Geol.* 637, 121674. doi:
1304 10.1016/j.chemgeo.2023.121674.

1305 Stumm, W., and Morgan, J. J. (1996). *Aquatic chemistry: chemical equilibria and rates in natural
1306 waters*. 3rd ed. New York: Wiley Available at:
1307 <http://catdir.loc.gov/catdir/toc/onix05/94048319.html> [Accessed October 24, 2023].

1308 Suhrhoff, T. J., Rickli, J., Christl, M., Vologina, E. G., Pham, V., Belhadj, M., et al. (2022). Source to
1309 sink analysis of weathering fluxes in Lake Baikal and its watershed based on riverine fluxes,
1310 elemental lake budgets, REE patterns, and radiogenic (Nd, Sr) and 10Be/9Be isotopes.
1311 *Geochim. Cosmochim. Acta* 321, 133–154. doi: 10.1016/j.gca.2022.01.007.

1312 Swoboda, P., Döring, T. F., and Hamer, M. (2022). Remineralizing soils? The agricultural usage of
1313 silicate rock powders: A review. *Sci. Total Environ.* 807, 150976. doi:
1314 10.1016/j.scitotenv.2021.150976.

1315 Taylor, L. L., Driscoll, C. T., Groffman, P. M., Rau, G. H., Blum, J. D., and Beerling, D. J. (2021).
1316 Increased carbon capture by a silicate-treated forested watershed affected by acid deposition.
1317 *Biogeosciences* 18, 169–188. doi: 10.5194/bg-18-169-2021.

1318 Taylor, L. L., Quirk, J., Thorley, R. M. S., Kharecha, P. A., Hansen, J., Ridgwell, A., et al. (2016).
1319 Enhanced weathering strategies for stabilizing climate and averting ocean acidification. *Nat.
1320 Clim. Change* 6, 402–406. doi: 10.1038/nclimate2882.

1321 te Pas, E. E. E. M., Hagens, M., and Comans, R. N. J. (2023). Assessment of the enhanced weathering
1322 potential of different silicate minerals to improve soil quality and sequester CO₂. *Front. Clim.*
1323 4. doi: 10.3389/fclim.2022.954064.

1324 Teng, F.-Z., Dauphas, N., and Watkins, J. M. (2017). Non-Traditional Stable Isotopes: Retrospective
1325 and Prospective. *Rev. Mineral. Geochem.* 82, 1–26. doi: 10.2138/rmg.2017.82.1.

1326 Tessier, A., Campbell, P. G., and Bisson, M. (1979). Sequential extraction procedure for the speciation
1327 of particulate trace metals. *Anal. Chem.* 51, 844–851.

1328 Thomas, M., and Reid, R. (2021). Vacuolar compartmentalisation and efflux of cadmium in barley.
1329 *Botany* 99, 1–8.

1330 USGS (2019). National Field Manual for the Collection of Water-Quality Data (NFM) | U.S.
1331 Geological Survey. Available at:
1332 <https://www.usgs.gov/mission-areas/water-resources/science/national-field-manual-collection>
1333 [-water-quality-data-nfm](https://www.usgs.gov/mission-areas/water-resources/science/national-field-manual-collection) [Accessed October 27, 2023].

1334 Vienne, A., Frings, P., Poblador, S., Steinwider, L., Rijnders, J., Schoelynck, J., et al. (2023). Soil
1335 Carbon Sequestration and the Role of Earthworms in an Enhanced Weathering Mesocosm
1336 Experiment. *Available SSRN 4449286*. doi: <https://dx.doi.org/10.2139/ssrn.4449286>.

1337 Vienne, A., Poblador, S., Portillo-Estrada, M., Hartmann, J., Ijehon, S., Wade, P., et al. (2022).
1338 Enhanced Weathering Using Basalt Rock Powder: Carbon Sequestration, Co-benefits and
1339 Risks in a Mesocosm Study With *Solanum tuberosum*. *Front. Clim.* 4. Available at:
1340 <https://www.frontiersin.org/articles/10.3389/fclim.2022.869456> [Accessed October 16, 2023].

1341 Viers, J., Oliva, P., Dandurand, J.-L., Dupré, B., and Gaillardet, J. (2007). “5.20 - Chemical
1342 Weathering Rates, CO₂ Consumption, and Control Parameters Deduced from the Chemical
1343 Composition of Rivers,” in *Treatise on Geochemistry*, eds. H. D. Holland and K. K. Turekian
1344 (Oxford: Pergamon), 1–25. doi: 10.1016/B978-008043751-4/00249-2.

1345 Vink, J. P. M., Giesen, D., and Ahlrichs, E. (2022). Olivine weathering in field trials Effect of natural
1346 environmental conditions on mineral dissolution and the potential toxicity of nickel.

1347 Vogel, J. C. (1993). “4 - Variability of Carbon Isotope Fractionation during Photosynthesis,” in *Stable*
1348 *Isotopes and Plant Carbon-water Relations*, eds. J. R. Ehleringer, A. E. Hall, and G. D.
1349 Farquhar (San Diego: Academic Press), 29–46. doi: 10.1016/B978-0-08-091801-3.50010-6.

1350 Walker, J. C. G., Hays, P. B., and Kasting, J. F. (1981). A negative feedback mechanism for the
1351 long-term stabilization of Earth’s surface temperature. *J. Geophys. Res. Oceans* 86,
1352 9776–9782. doi: 10.1029/JC086iC10p09776.

1353 Weil, R., and Brady, N. (2017). *The Nature and Properties of Soils. 15th edition*.

1354 Wen, H., Sullivan, P. L., Billings, S. A., Ajami, H., Cueva, A., Flores, A., et al. (2022). From Soils to
1355 Streams: Connecting Terrestrial Carbon Transformation, Chemical Weathering, and Solute
1356 Export Across Hydrological Regimes. *Water Resour. Res.* 58, e2022WR032314. doi:
1357 10.1029/2022WR032314.

1358 West, A. J., Galy, A., and Bickle, M. (2005). Tectonic and climatic controls on silicate weathering.
1359 *Earth Planet. Sci. Lett.* 235, 211–228. doi: 10.1016/j.epsl.2005.03.020.

1360 Whitworth, T. M. (1998). “Clay minerals: ion exchange/Ion exchange,” in *Geochemistry Encyclopedia*
1361 *of Earth Science*. (Dordrecht: Springer Netherlands), 85–87. doi: 10.1007/1-4020-4496-8_56.

1362 Wolf, A., Chang, E., and Tank, A. (2023). Verification methods and agronomic enhancements for
1363 carbon removal based on enhanced rock weathering. Available at:
1364 <https://image-ppubs.uspto.gov/dirsearch-public/print/downloadPdf/11644454> [Accessed
1365 October 23, 2023].

1366 Wolf-Gladrow, D. A., Zeebe, R. E., Klaas, C., Körtzinger, A., and Dickson, A. G. (2007). Total
1367 alkalinity: The explicit conservative expression and its application to biogeochemical
1368 processes. *Mar. Chem.* 106, 287–300. doi: 10.1016/j.marchem.2007.01.006.

1369 Wood, C., Harrison, A. L., and Power, I. M. (2023). Impacts of dissolved phosphorus and
1370 soil-mineral-fluid interactions on CO₂ removal through enhanced weathering of wollastonite
1371 in soils. *Appl. Geochem.* 148, 105511. doi: 10.1016/j.apgeochem.2022.105511.

1372 Yan, Y., Dong, X., Li, R., Zhang, Y., Yan, S., Guan, X., et al. (2023). Wollastonite addition stimulates
1373 soil organic carbon mineralization: Evidences from 12 land-use types in subtropical China.
1374 *CATENA* 225, 107031. doi: 10.1016/j.catena.2023.107031.

1375 Zamanian, K., Pustovoytov, K., and Kuzyakov, Y. (2016). Pedogenic carbonates: Forms and formation
1376 processes. *Earth-Sci. Rev.* 157, 1–17. doi: 10.1016/j.earscirev.2016.03.003.

1377 Zeebe, R., and Wolf-Gladrow, D. (2001). CO₂ in Seawater: Equilibrium, Kinetics, Isotopes. in
1378 Available at:
1379 [https://www.semanticscholar.org/paper/CO2-in-Seawater%3A-Equilibrium%2C-Kinetics%2C](https://www.semanticscholar.org/paper/CO2-in-Seawater%3A-Equilibrium%2C-Kinetics%2C-Isotopes-Zeebe-Wolf-Gladrow/171c4a87efd2630eae567d92d2d9ece4541d980d)
1380 [-Isotopes-Zeebe-Wolf-Gladrow/171c4a87efd2630eae567d92d2d9ece4541d980d](https://www.semanticscholar.org/paper/CO2-in-Seawater%3A-Equilibrium%2C-Kinetics%2C-Isotopes-Zeebe-Wolf-Gladrow/171c4a87efd2630eae567d92d2d9ece4541d980d) [Accessed
1381 October 18, 2023].

1382 Zhang, B., Kroeger, J., Planavsky, N., and Yao, Y. (2023). Techno-Economic and Life Cycle
1383 Assessment of Enhanced Rock Weathering: A Case Study from the Midwestern United
1384 States. *Environ. Sci. Technol.* 57, 13828–13837. doi: 10.1021/acs.est.3c01658.

1385 Zhang, S., Planavsky, N. J., Katchinoff, J., Raymond, P. A., Kanzaki, Y., Reershemius, T., et al.
1386 (2022). River chemistry constraints on the carbon capture potential of surficial enhanced rock
1387 weathering. *Limnol. Oceanogr.* 67, S148–S157. doi: 10.1002/lno.12244.